Understanding the observed properties of interstellar filaments

Insights on the initial conditions of star formation

Doris Arzoumanian (Nagoya University)

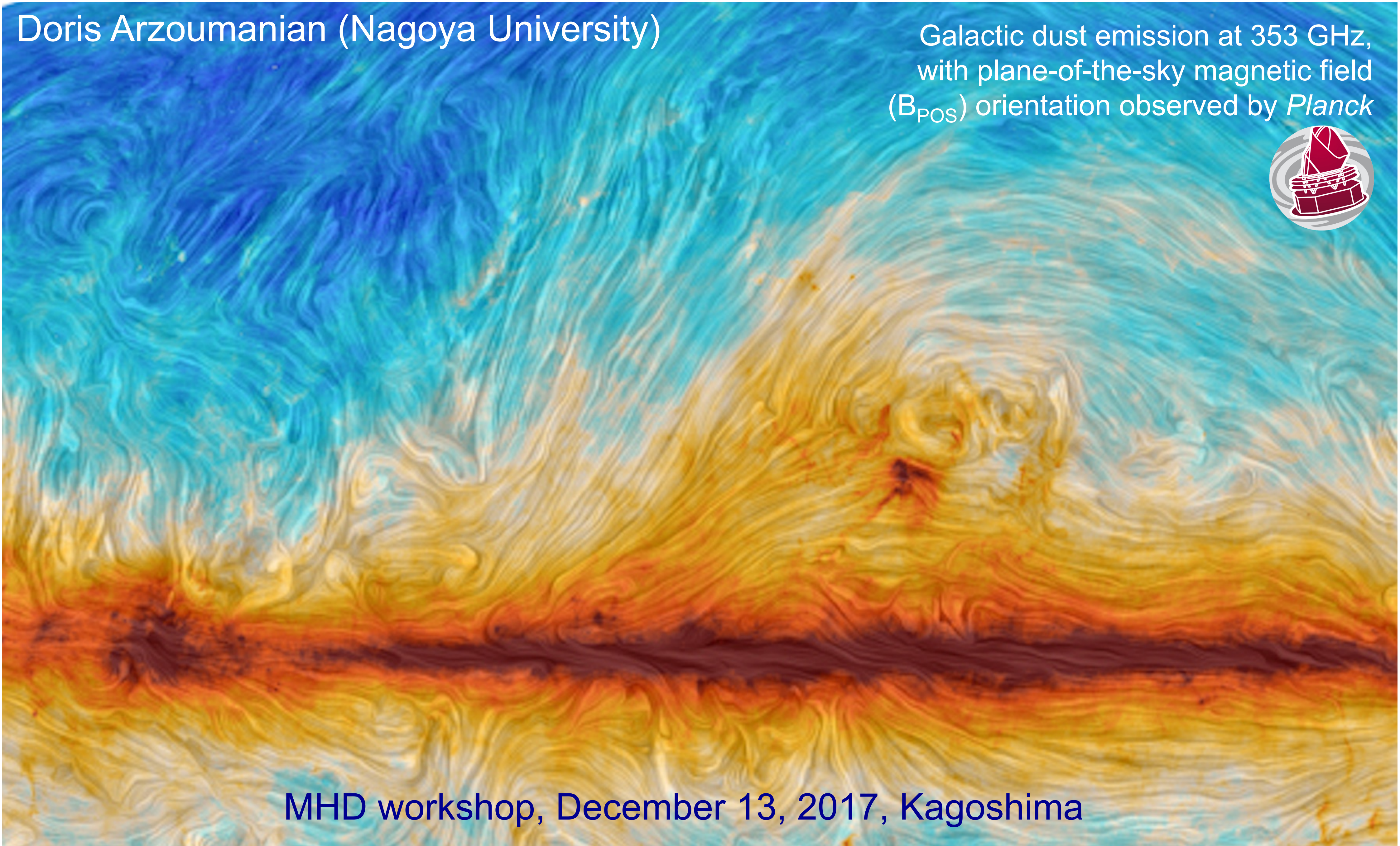

Galactic dust emission at 353 GHz, with plane-of-the-sky magnetic field (B_{POS}) orientation observed by *Planck*

MHD workshop, December 13, 2017, Kagoshima

Understanding the observed properties of interstellar filaments

Insights on the initial conditions of star formation

Galactic dust emission at 353 GHz, with plane-of-the-sky magnetic field (B_{POS}) orientation observed by *Planck*

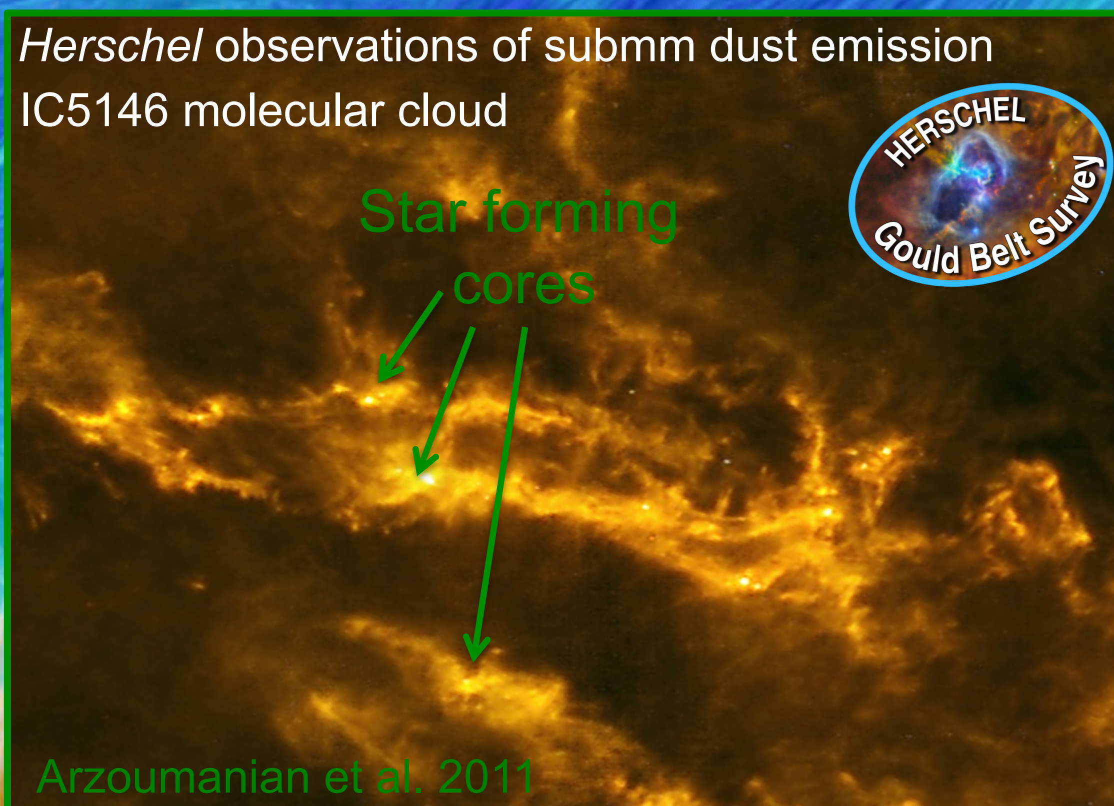

Outline

- Filament properties derived from dust continuum observations
- Kinematics of clouds and filaments from molecular line observations
- Insight on the magnetic field structure from dust polarization observations

Special thanks to
Shu-ichiro Inutsuka
Tsuyoshi Inoue
Yoshito Shimajiri
Philippe André

Doris Arzoumanian, MHD workshop, December 13, 2017, Kagoshima

Interstellar filaments share a common inner width of 0.1pc while they span a wide range in column density

Arzoumanian et al. 2011,+ in prep.

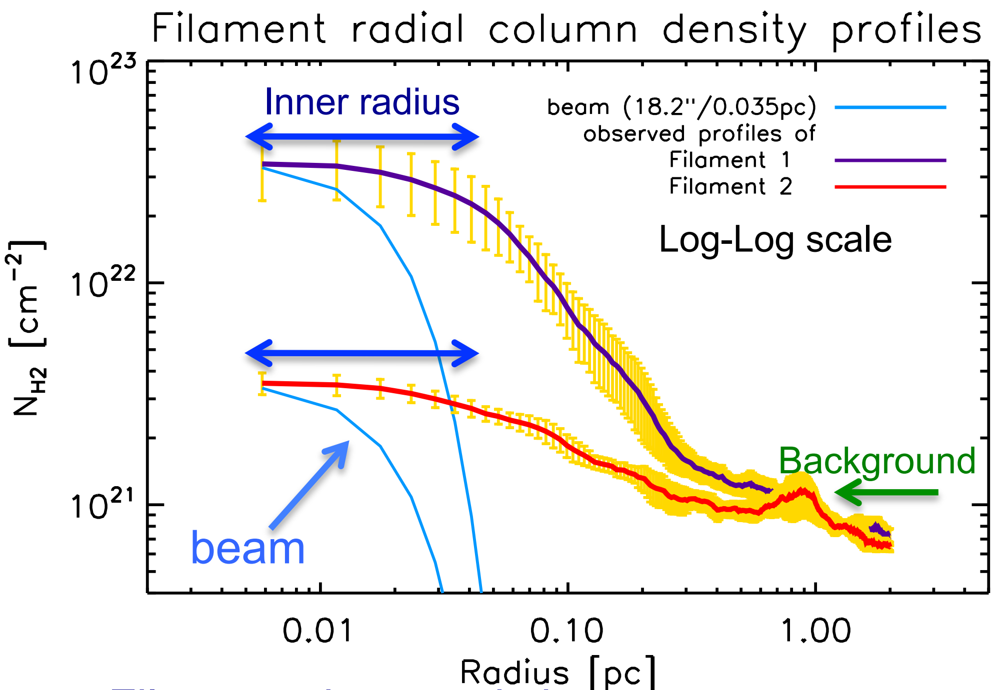

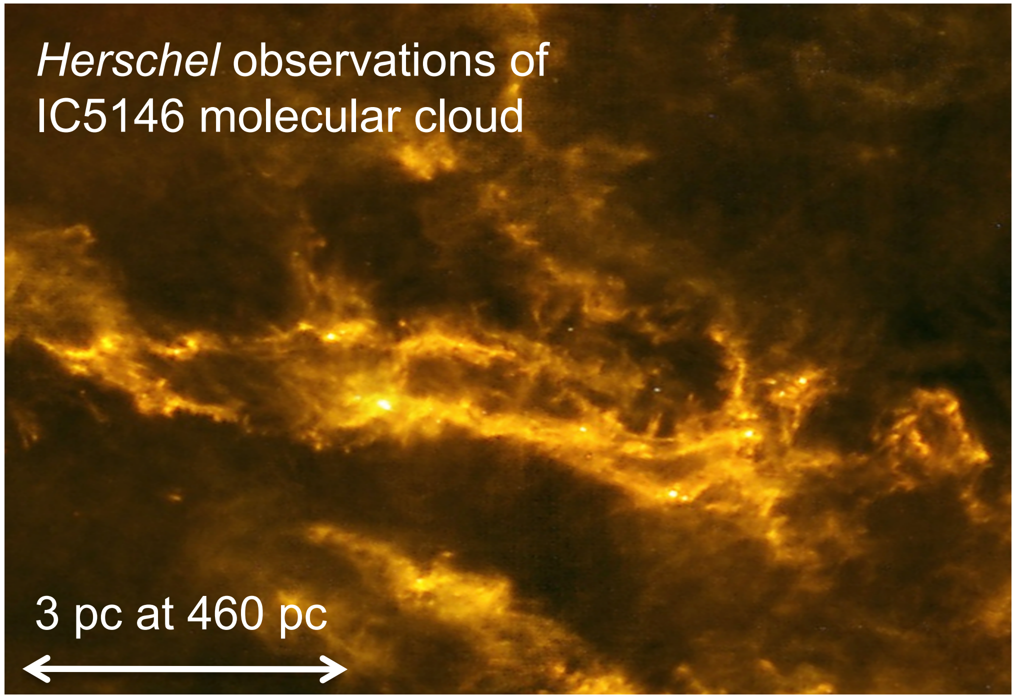

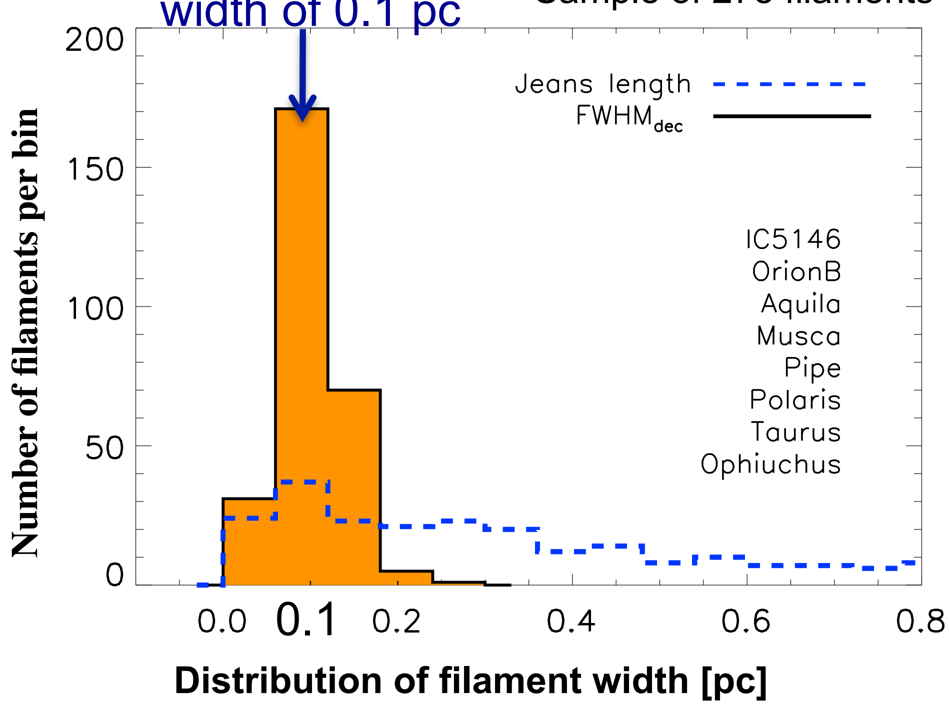

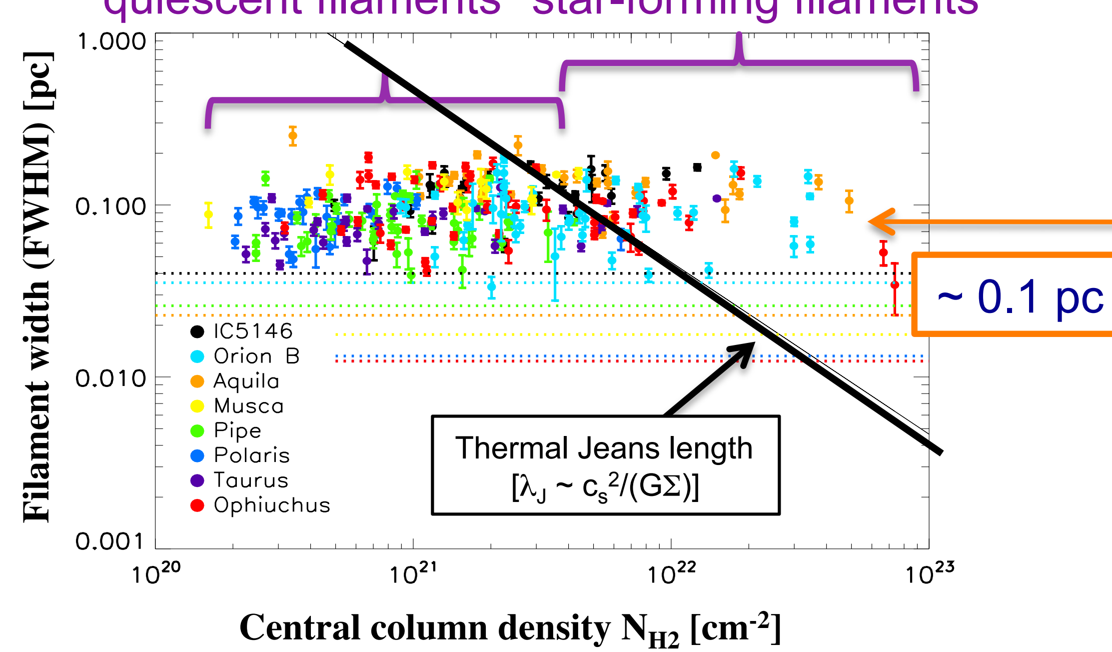

Doris Arzoumanian, MHD workshop, December 13, 2017, Kagoshima

Combining *Herschel* data with high resolution observations of ArTéMiS/APEX

×3.4 higher resolution than *Hersche* SPIRE
Open to ESO/OSO community since 2014

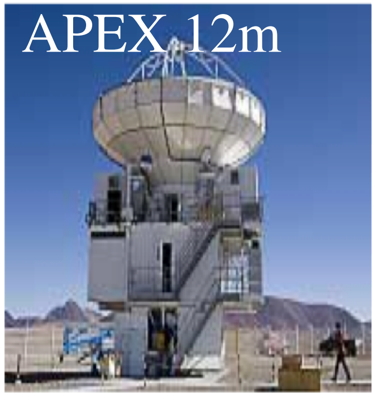

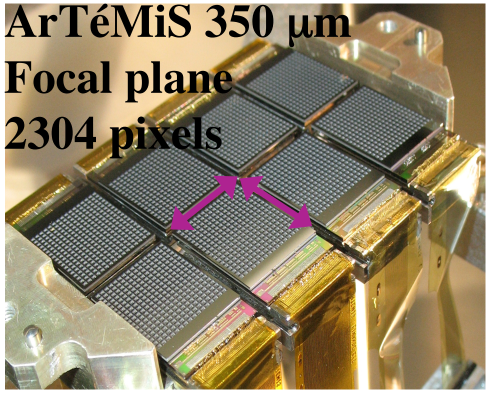

Observations (June 2016) of Serpens South in the Aquila rift

André, Revéret, Könyves, Shimajiri et al.

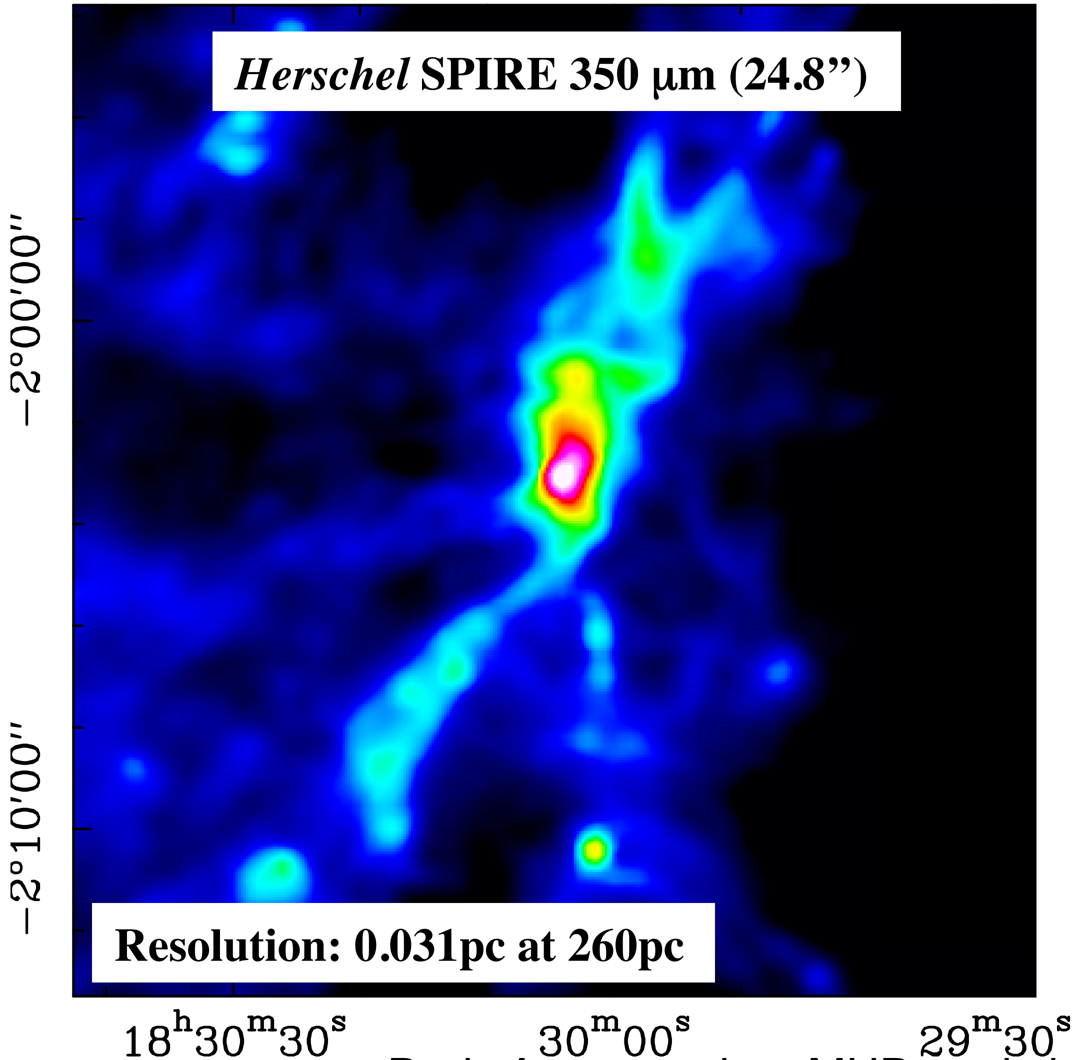

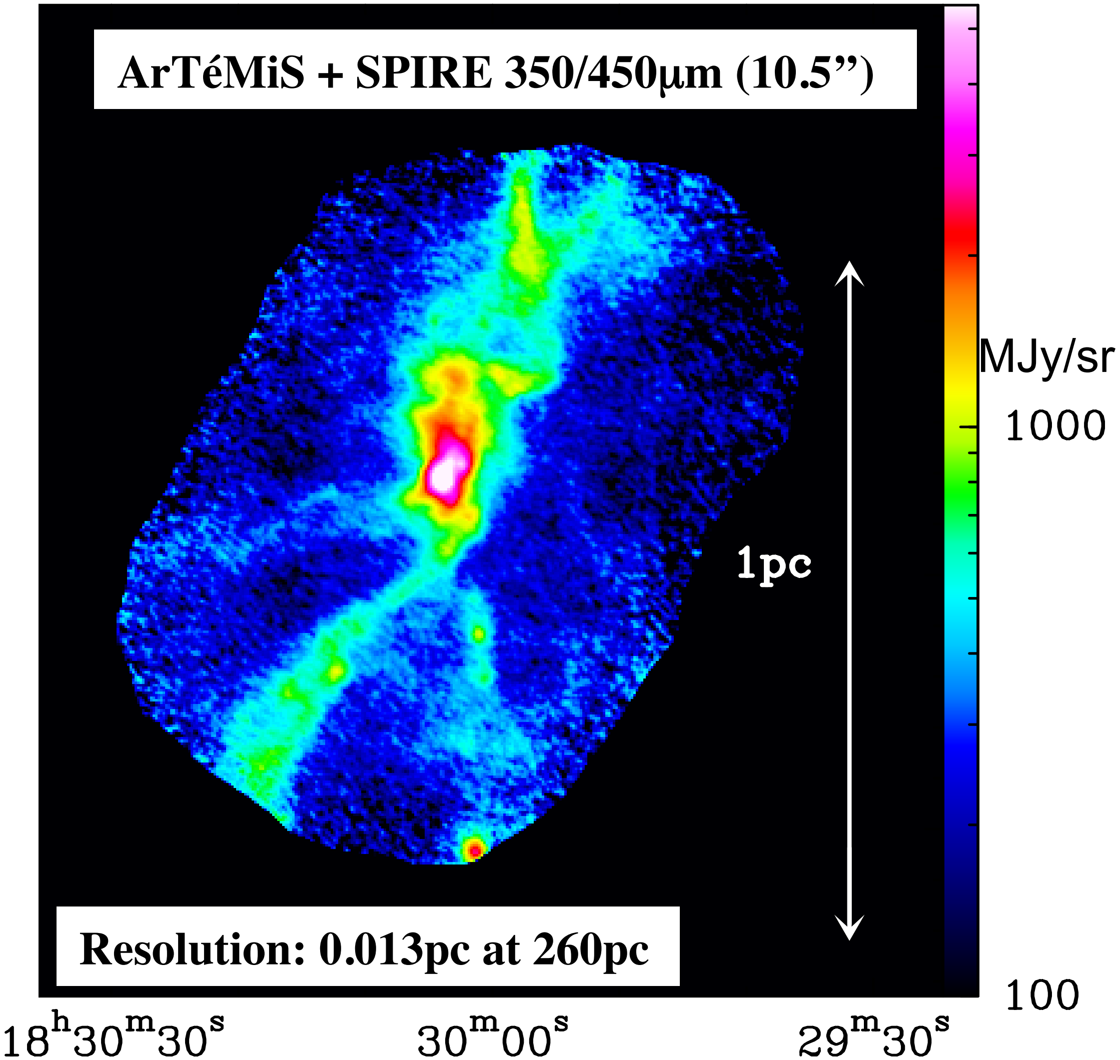

Combining *Herschel* data with high resolution observations of ArTéMiS/APEX

Recent observations (June 2016) of Serpens South in the Aquila rift

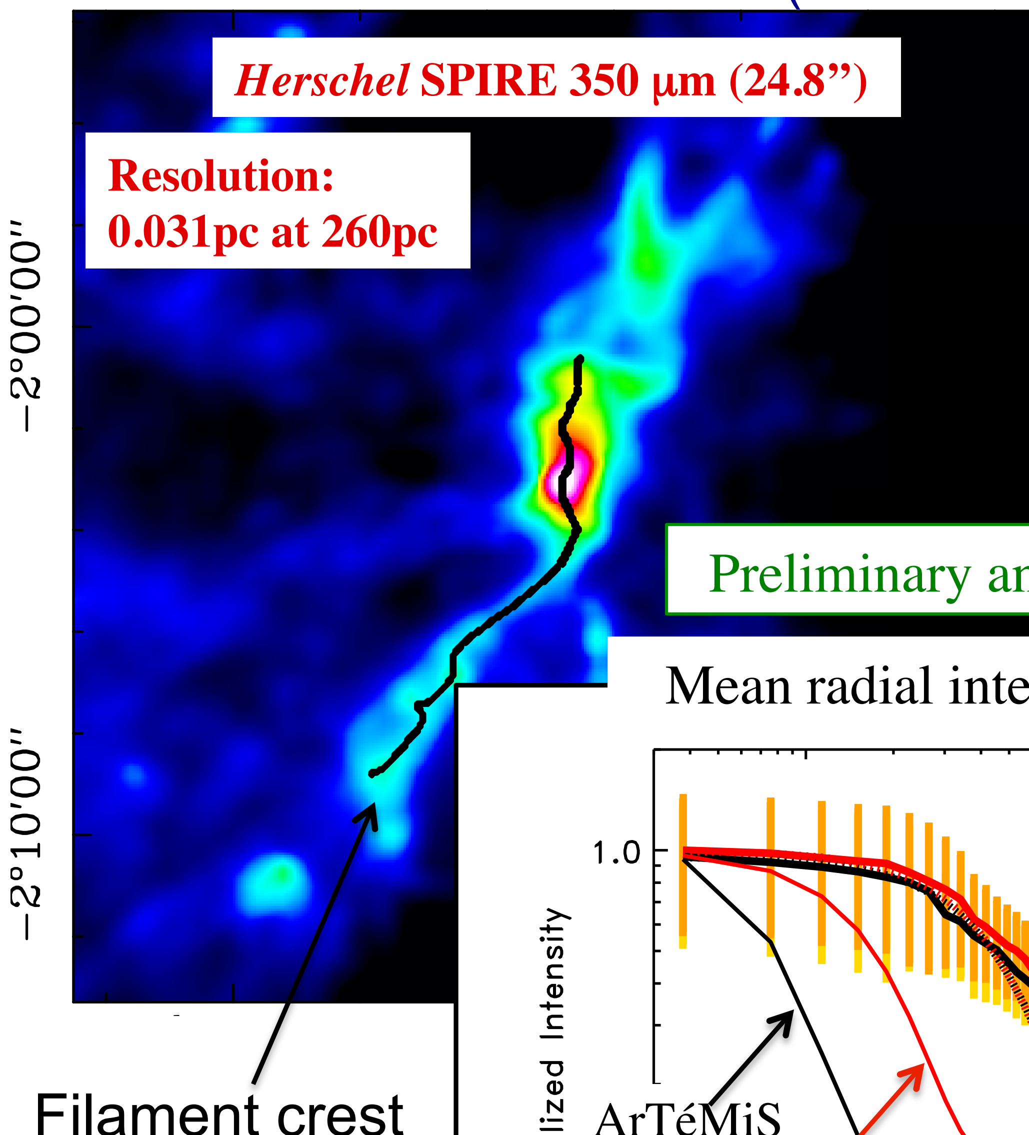

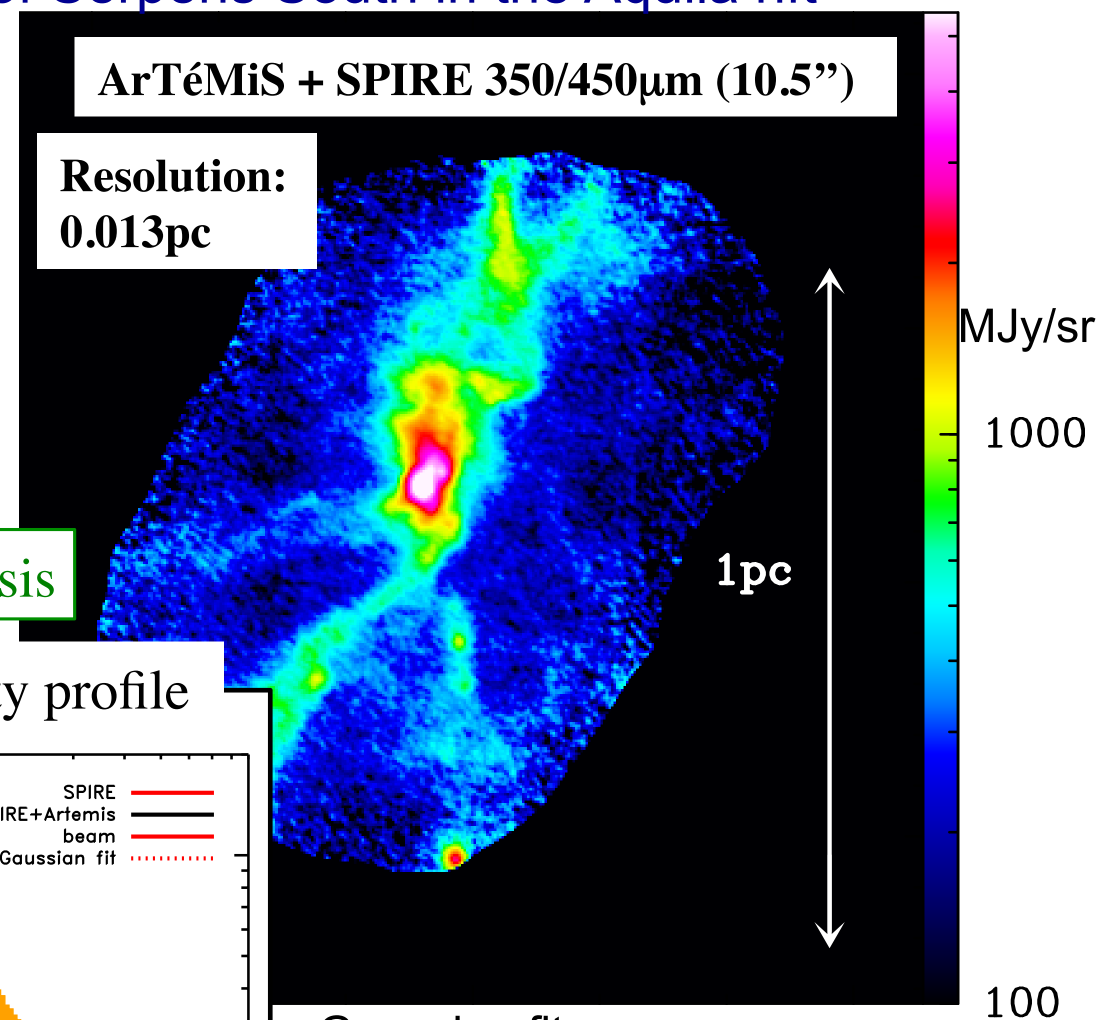

Preliminary analysis

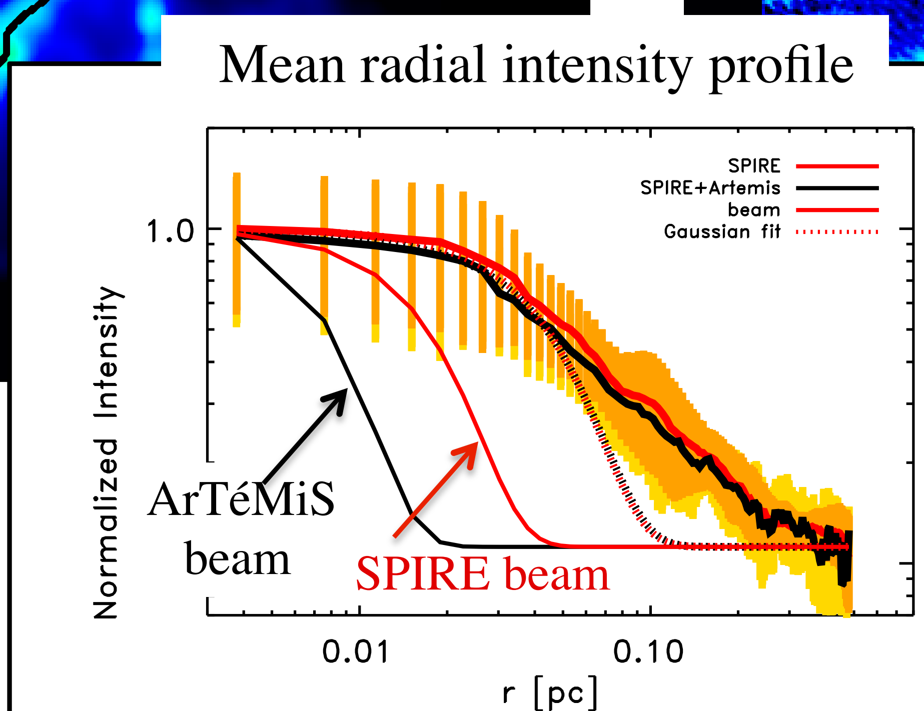

Gaussian fits:

FWHM = 0.083+- 0.012pc

FWHM = 0.087+- 0.013pc

$FWHM_{dec}$= 0.083+- 0.013pc

$FWHM_{dec}$= 0.081+- 0.013pc

Resolving the inner structure of filaments at distances further than the Gould Belt clouds

Combining *Herschel* data with high resolution observations with ArTéMiS/APEX 12m

André, Revéret, Könyves, Arzoumanian et al. 2016

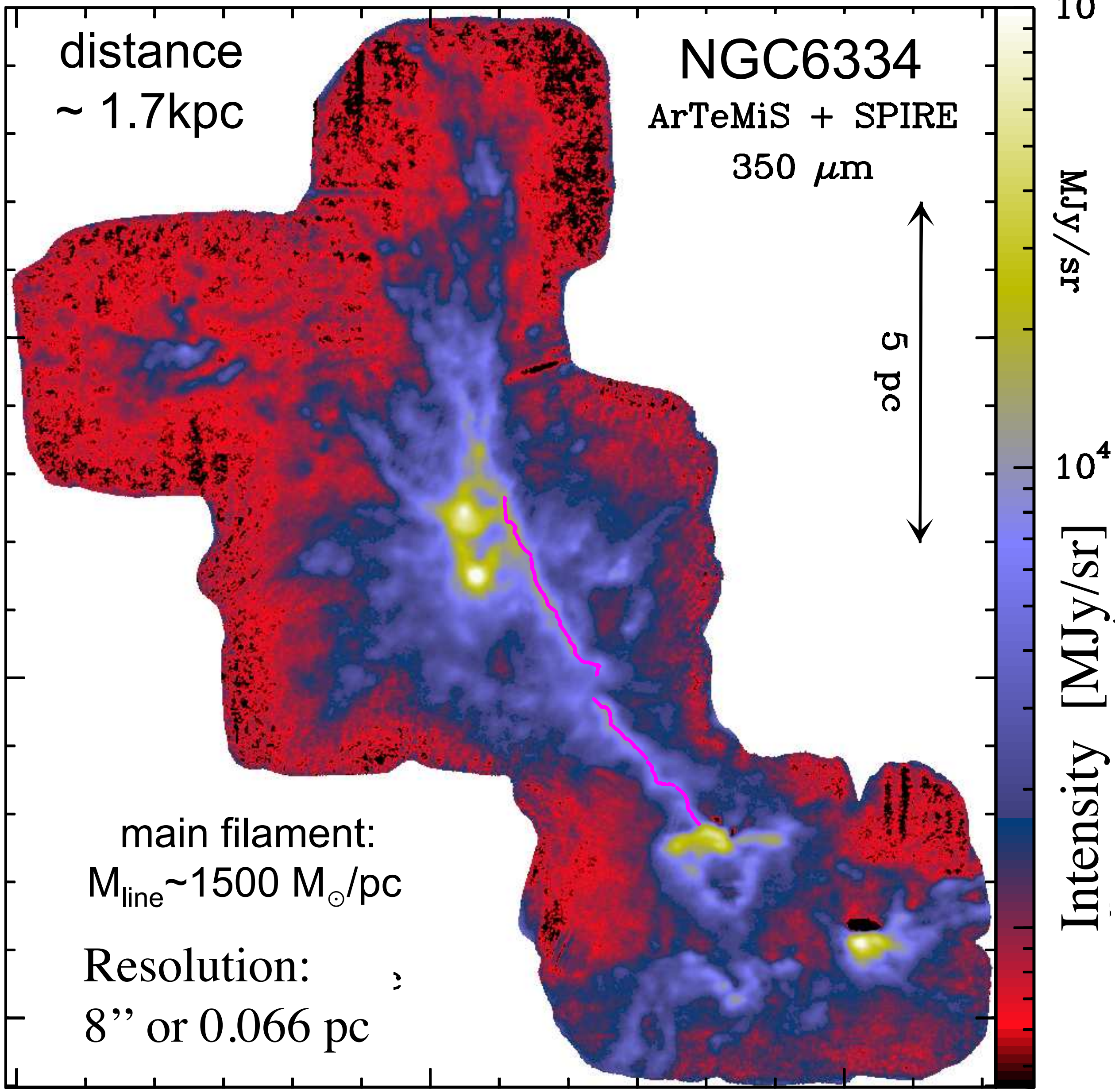

×3.4 higher resolution than *Hersche* SPIRE

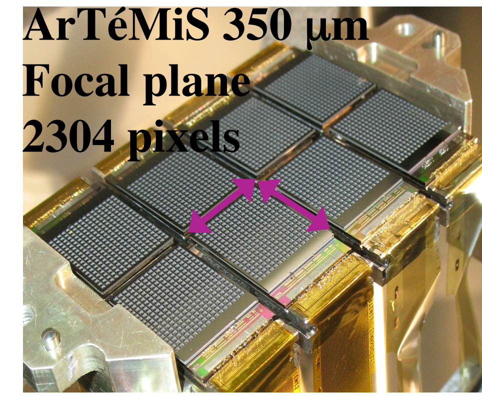

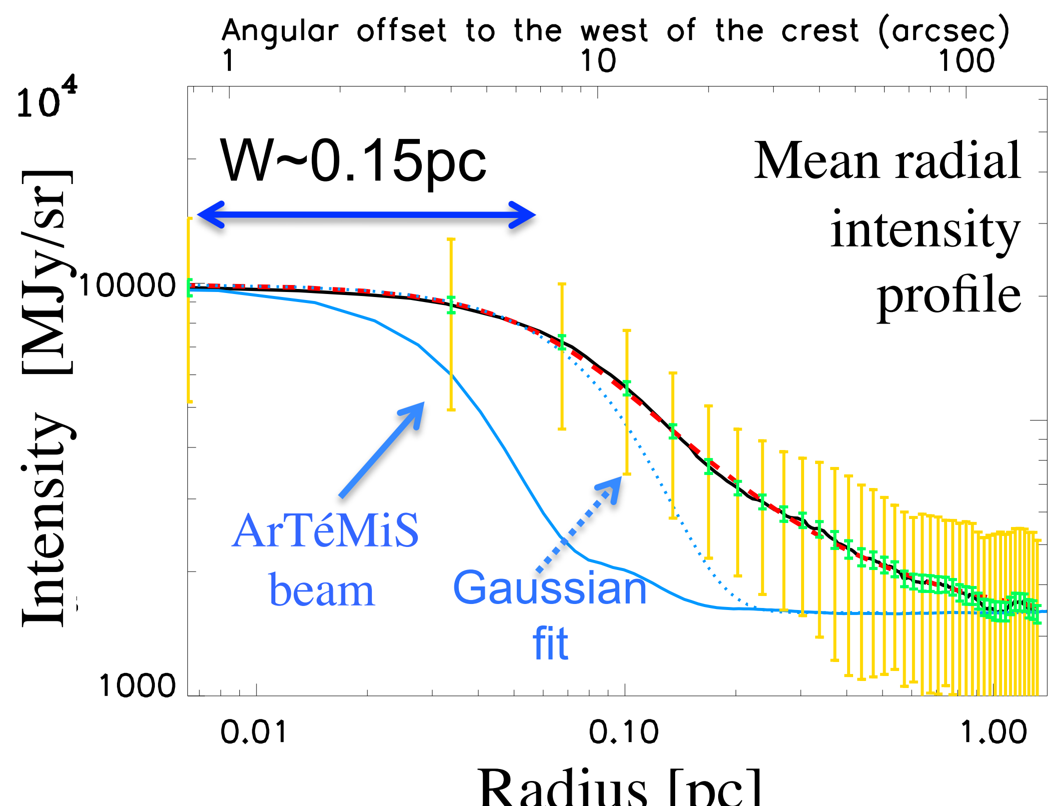

Filaments are also observed to be main structures of the interstellar medium of other galaxies

ALMA observations of pc-scale filaments in the LMC

Fukui et al. 2015, Tokuda et al., in prep.

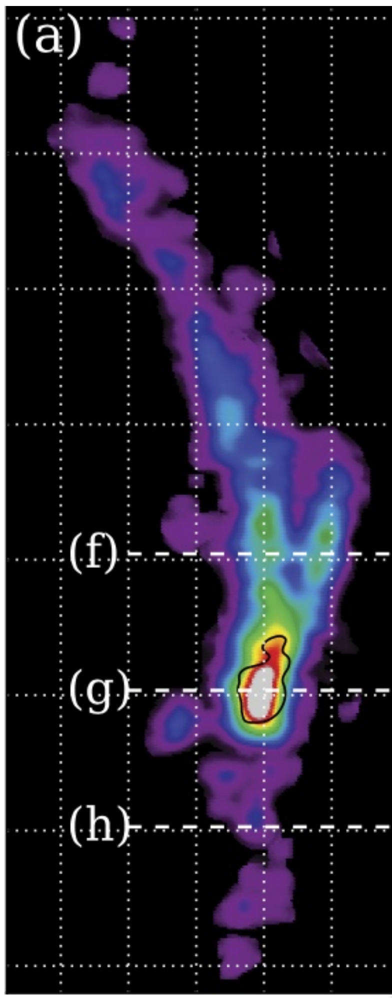

5 pc

Res. ~1”
~0.24pc
at 50kpc

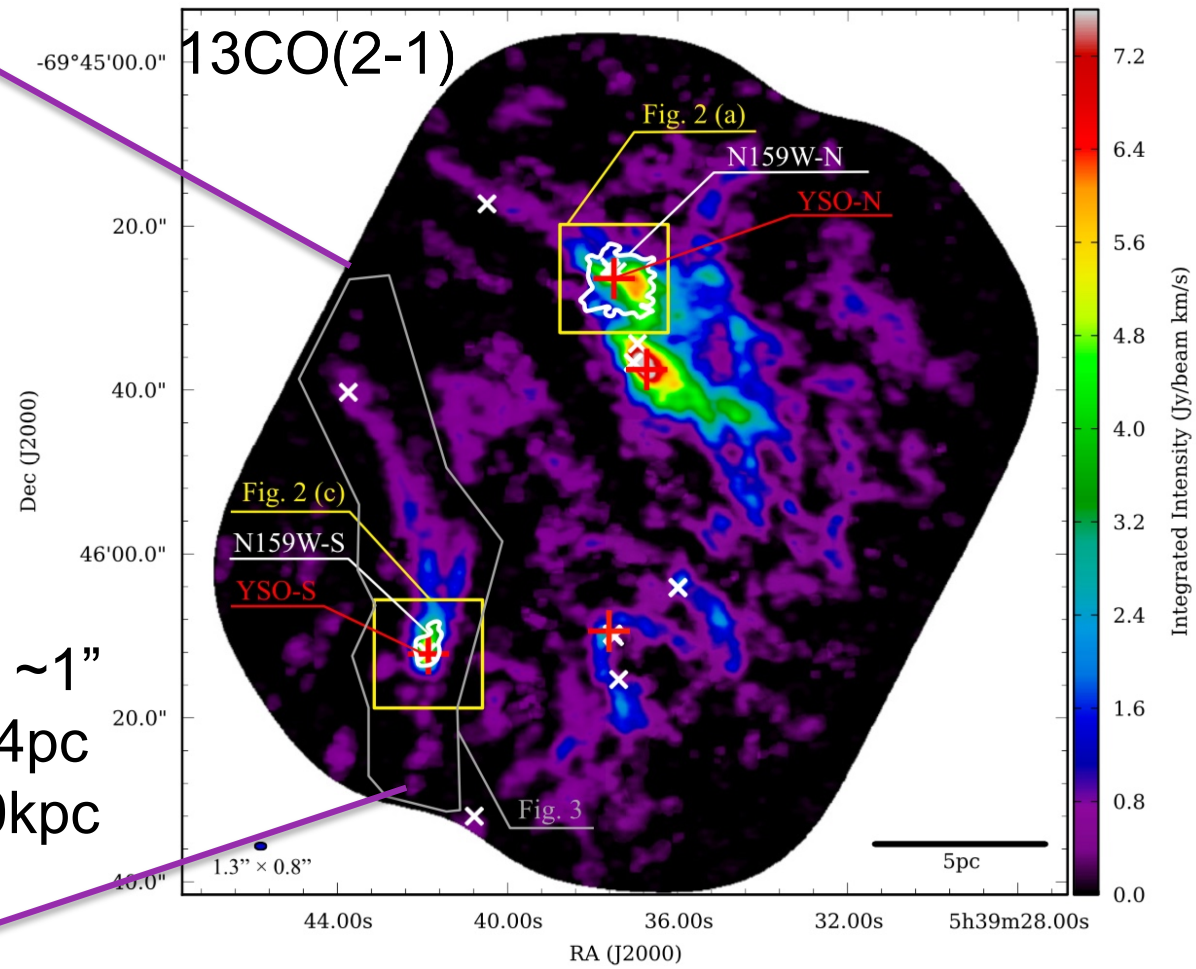

Filaments may help understanding the initial conditions of star formation in galaxies (cf. Lada et al. 2012)

Understanding the observed properties: Model of non isothermal filaments in pressure equilibrium with the ambient medium

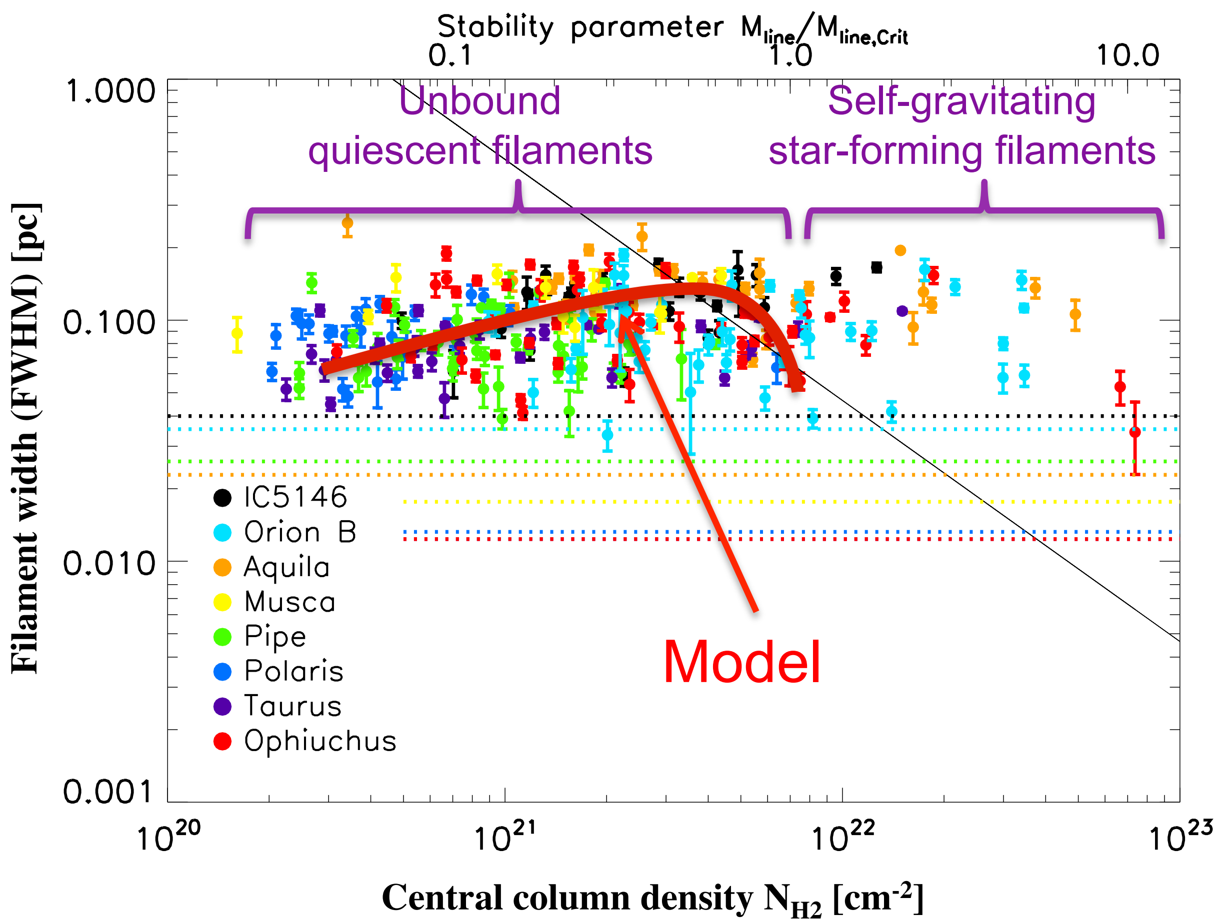

Model of polytropic filaments
$P \sim \rho^{\gamma}$
with
$\gamma = 0.8$ and
$P_{ex} / k_B \sim 5 \times 10^4$ K cm^{-3}

Reasonable agreement with the observations for subcritical filaments

(Inutsuka et al. in prep.)

Cf. Fischera & Martin 2012 for a model of isothermal filaments

Tension between filament models and observations

- Thermally supercritical filament with $M_{line} > M_{line,crit}$ are unstable for radial collapse and gravitational fragmentation (Inutsuka & Miyama 1992, 1997)
- Runaway collapse of thermally supercritical filaments with $M_{line} > 2M_{line,crit}$

Star forming supercritical filaments with $M_{line} >> 2M_{line,crit}$ are observed

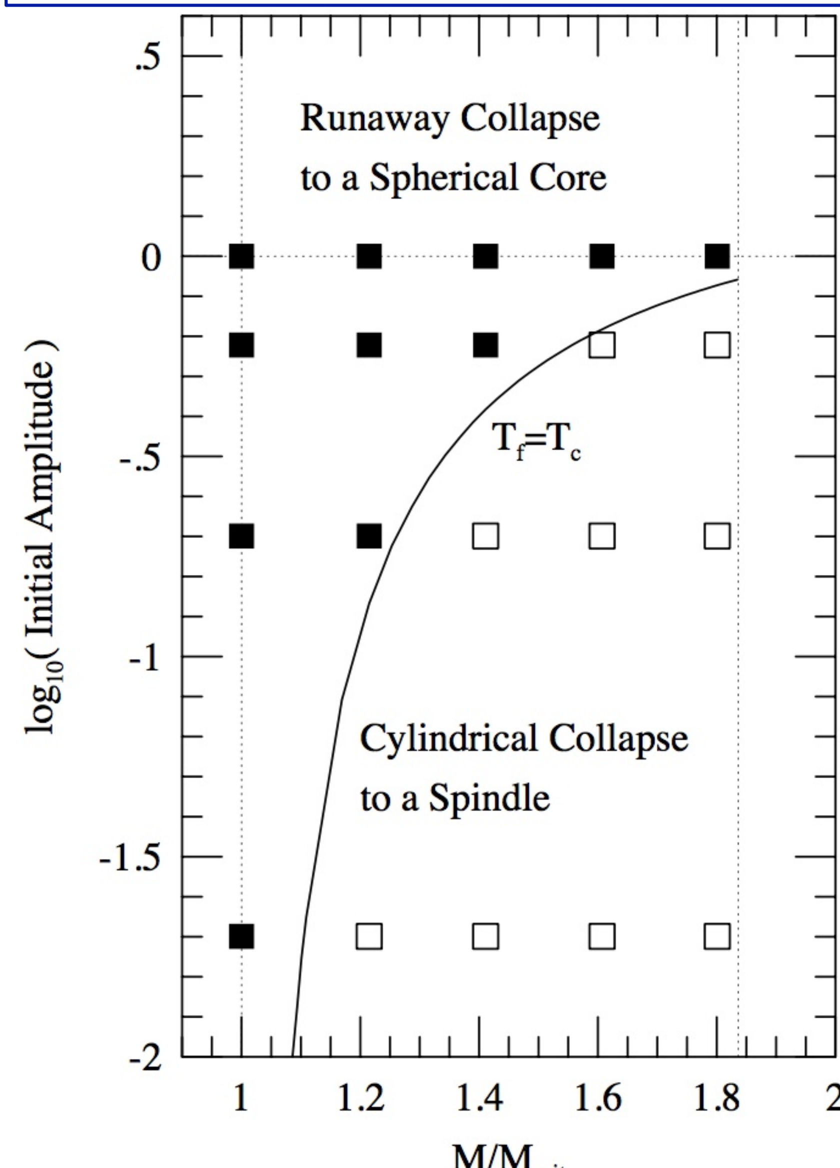

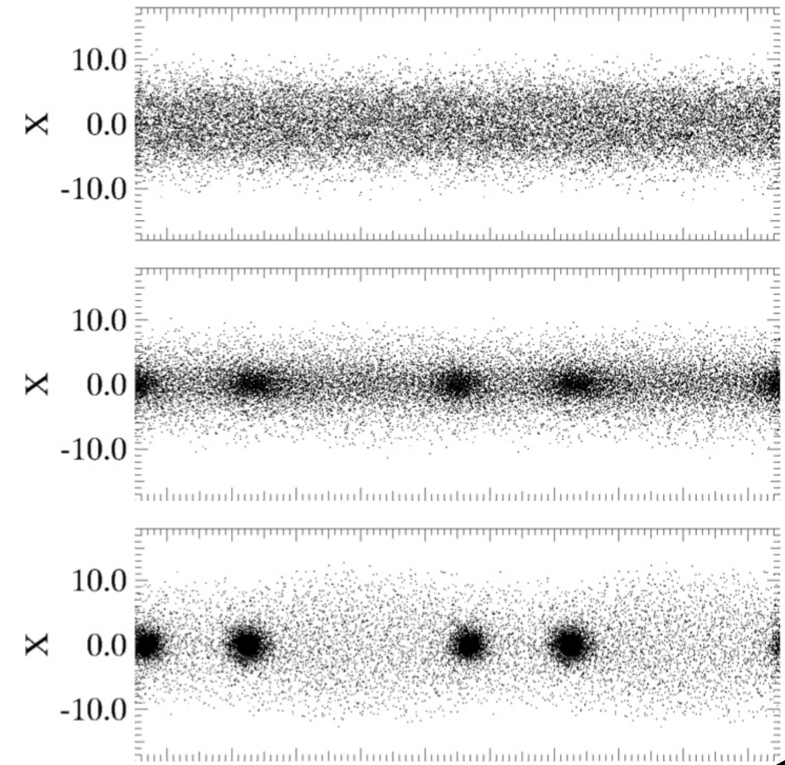

(Inutsuka & Miyama 1997)

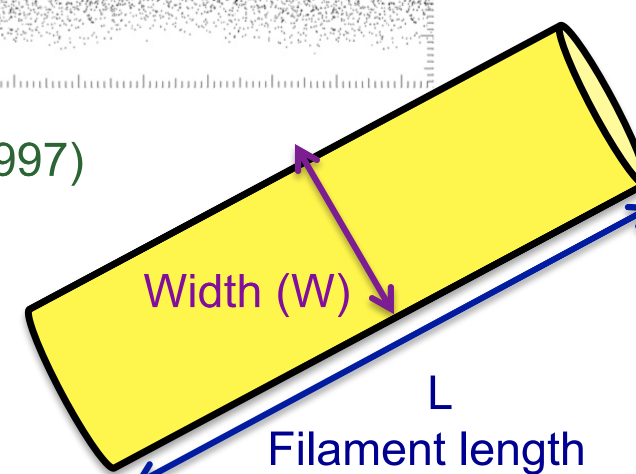

M_{line}=M/L

Understanding the observed properties: Model of accreting dense/self-gravitating filaments

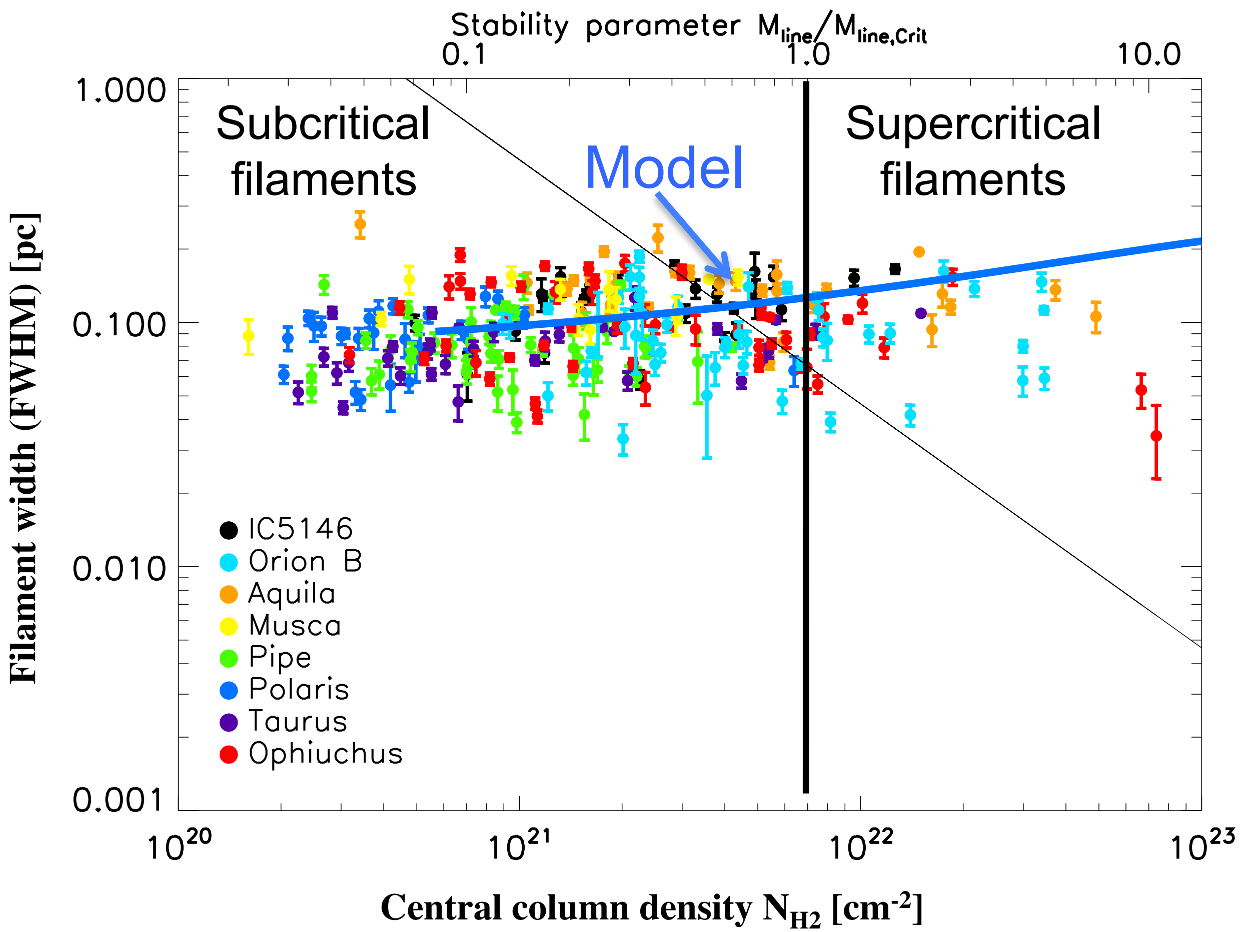

Balance between accretion-driven turbulence (Klessen & Hennebelle 2010) and dissipation of turbulence due to ion-neutral friction (Hennebelle & André 2013)

See also numerical simulations of gravitational infall onto molecular filaments (Heitsch 2013)

Hint of the evolution of supercritical filaments from Accretion of surrounding material channeled by the magnetic field?

Low column density filaments/striations aligned with the magnetic field seem to be feeding the dense filament

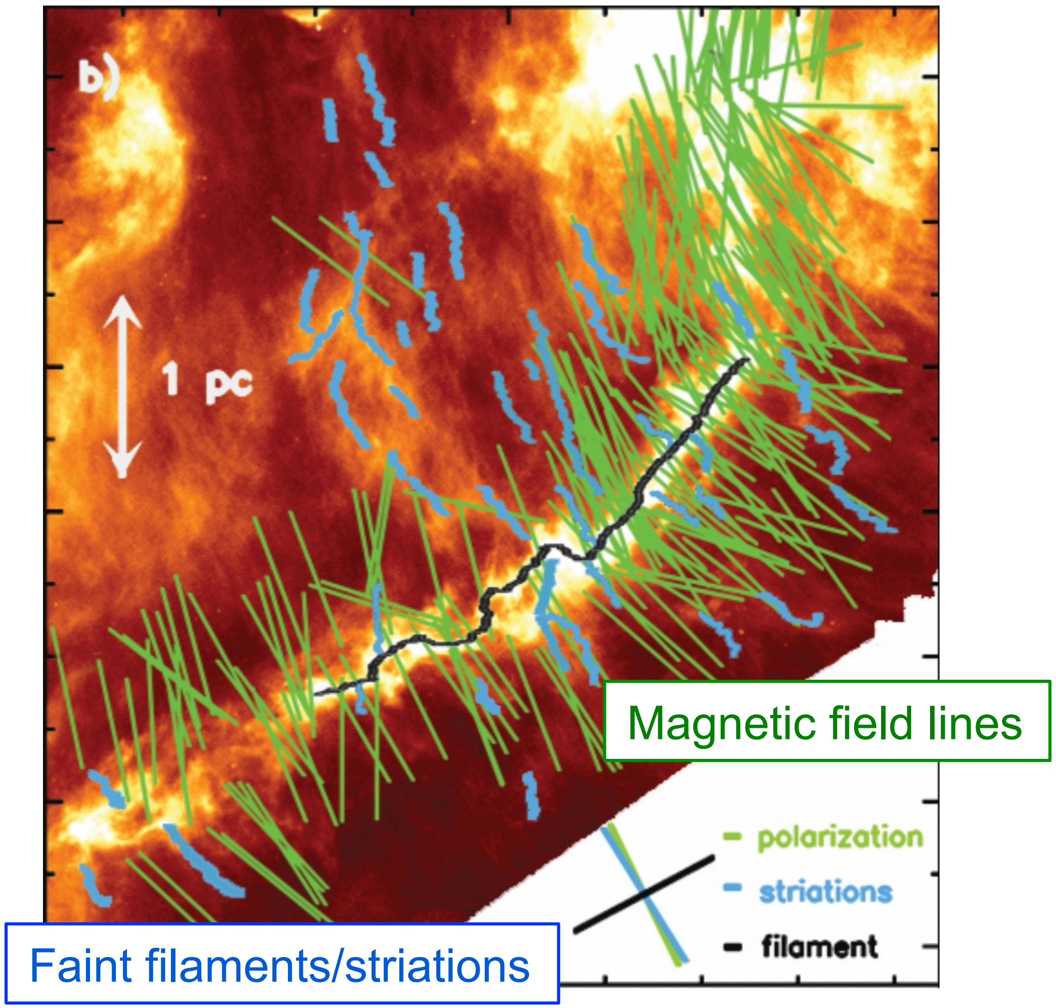

Herschel column density map (Palmeirim et al. 2013)

Magnetic field orientation from Optical/IR polarization (Heyer et al. 2008, Heils 2000, Chapman et al. 2011)

Red-shifted and blue-shifted velocity gradients on both sides of the filament trace flows of surrounding matter being accreted onto the filament?

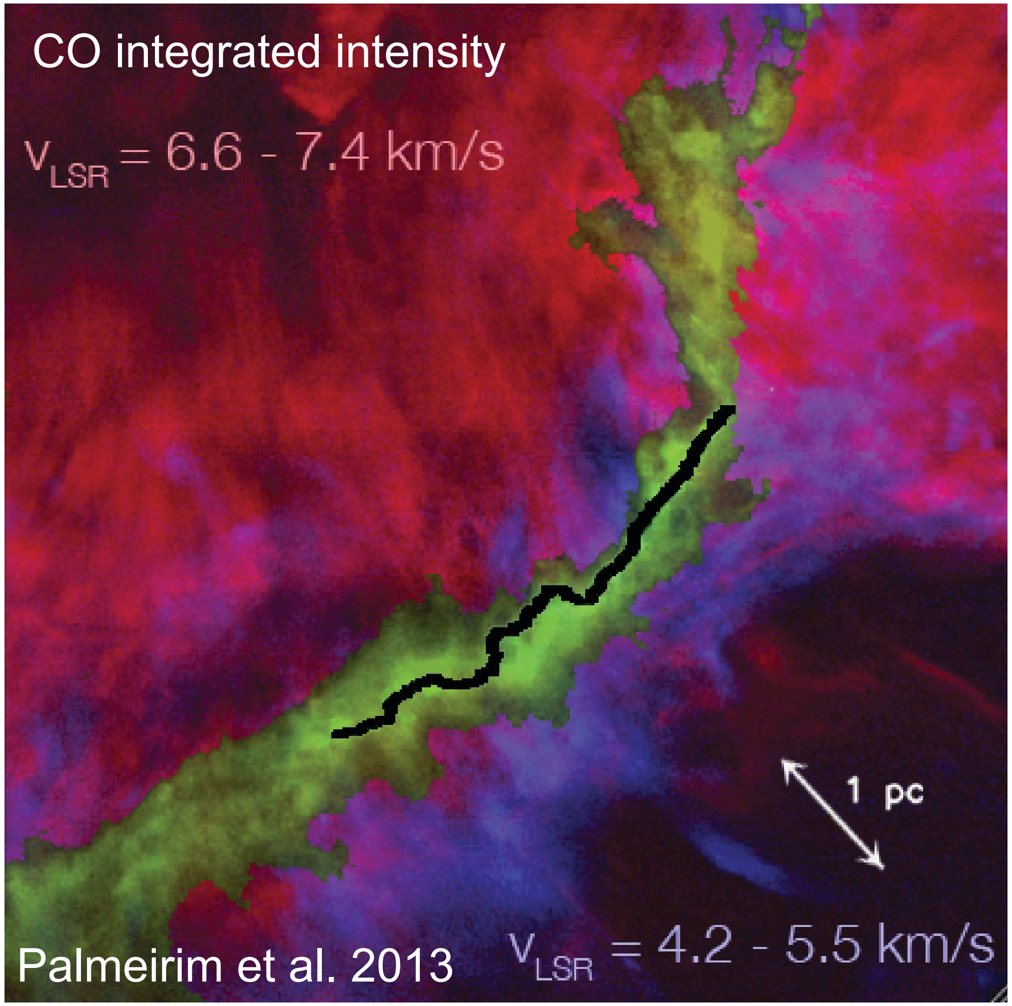

CO observations from Goldsmith et al. 2008

Doris Arzoumanian, MHD workshop, December 13, 2017, Kagoshima

Internal velocity structure of the B211/3 filament

"Velocity coherent filaments/fibers" observed along the B211/13 filament

Palmeirim et al. 2013

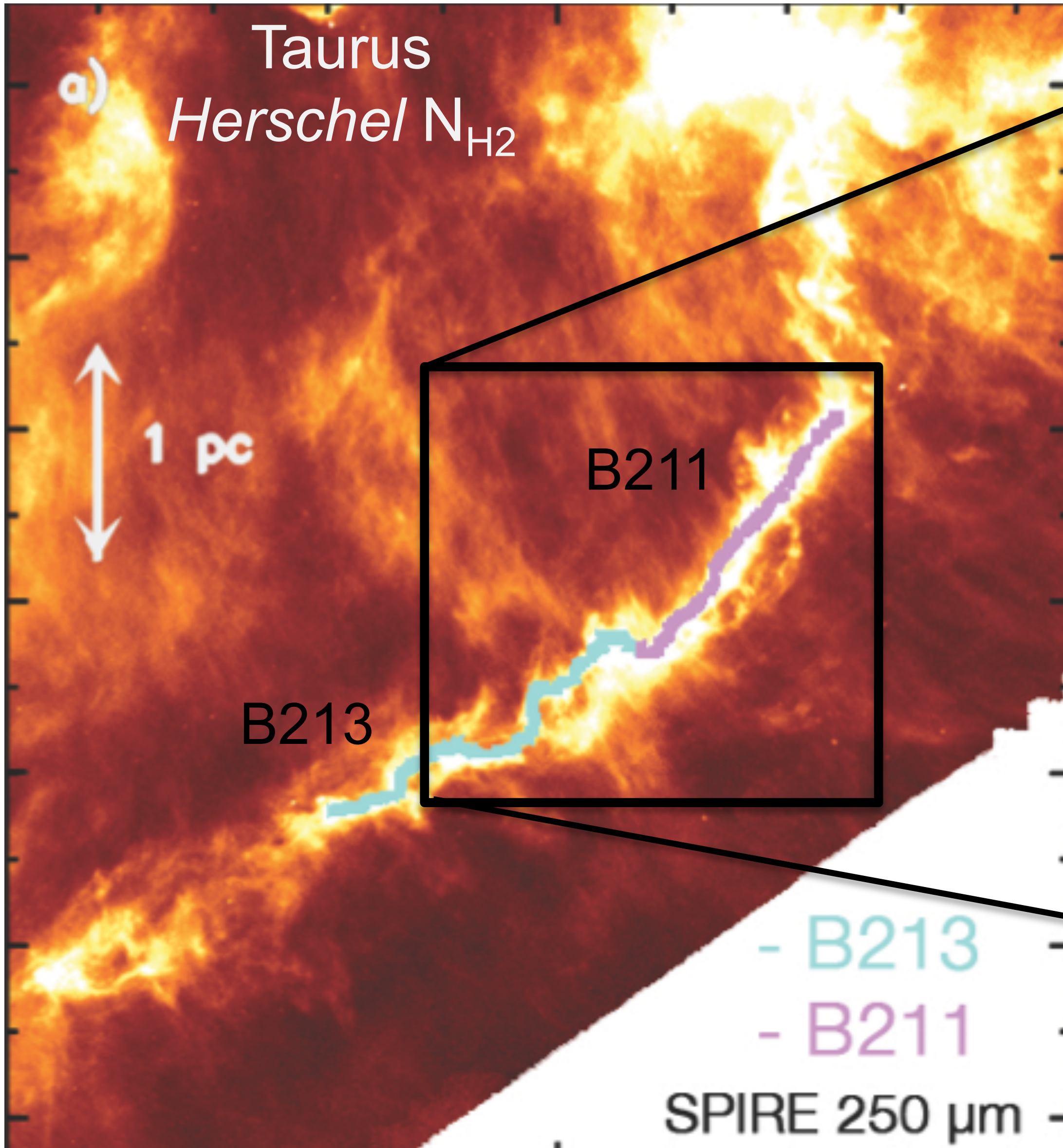

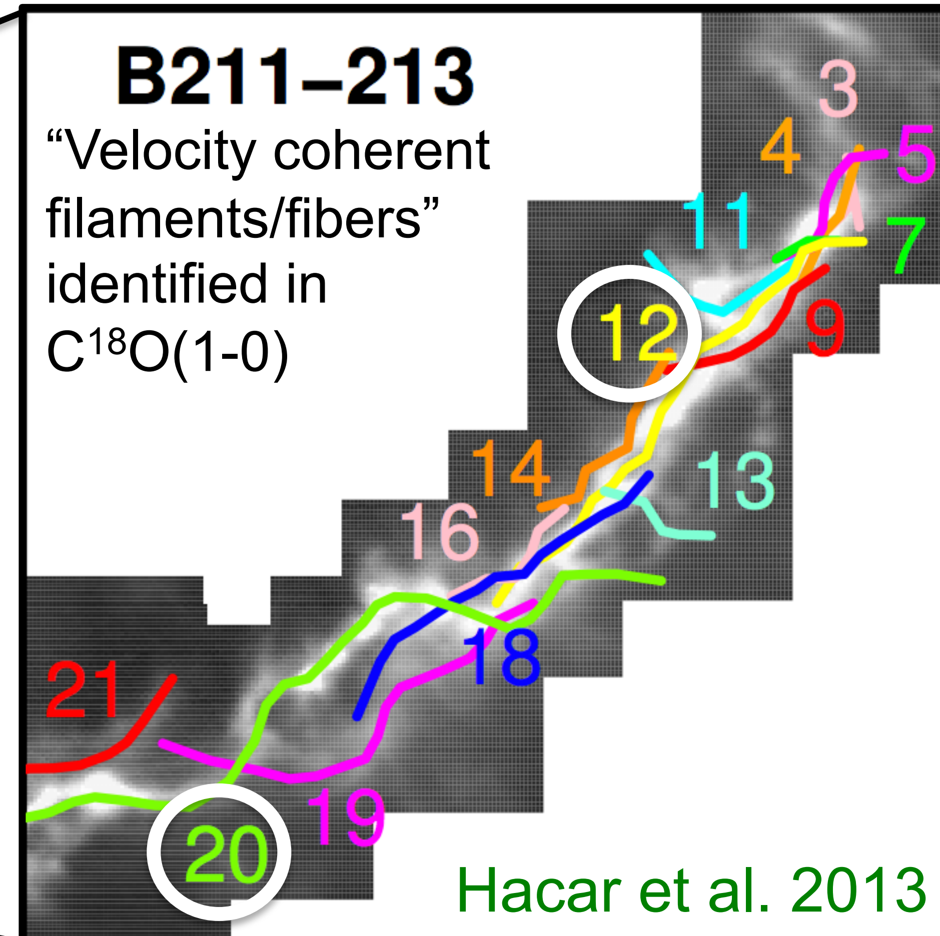

Fiber 12 traces the crest of B211
Fiber 20 traces the crest of B213

Possible scenario: Matter accretion in a turbulent flow can produce fiber-like structures and delay the global radial collapse of the supercritical filament (Clarke, Whitworth et al. 2017)

“Velocity coherent filaments/fibers” observed along the B211/13 filament?

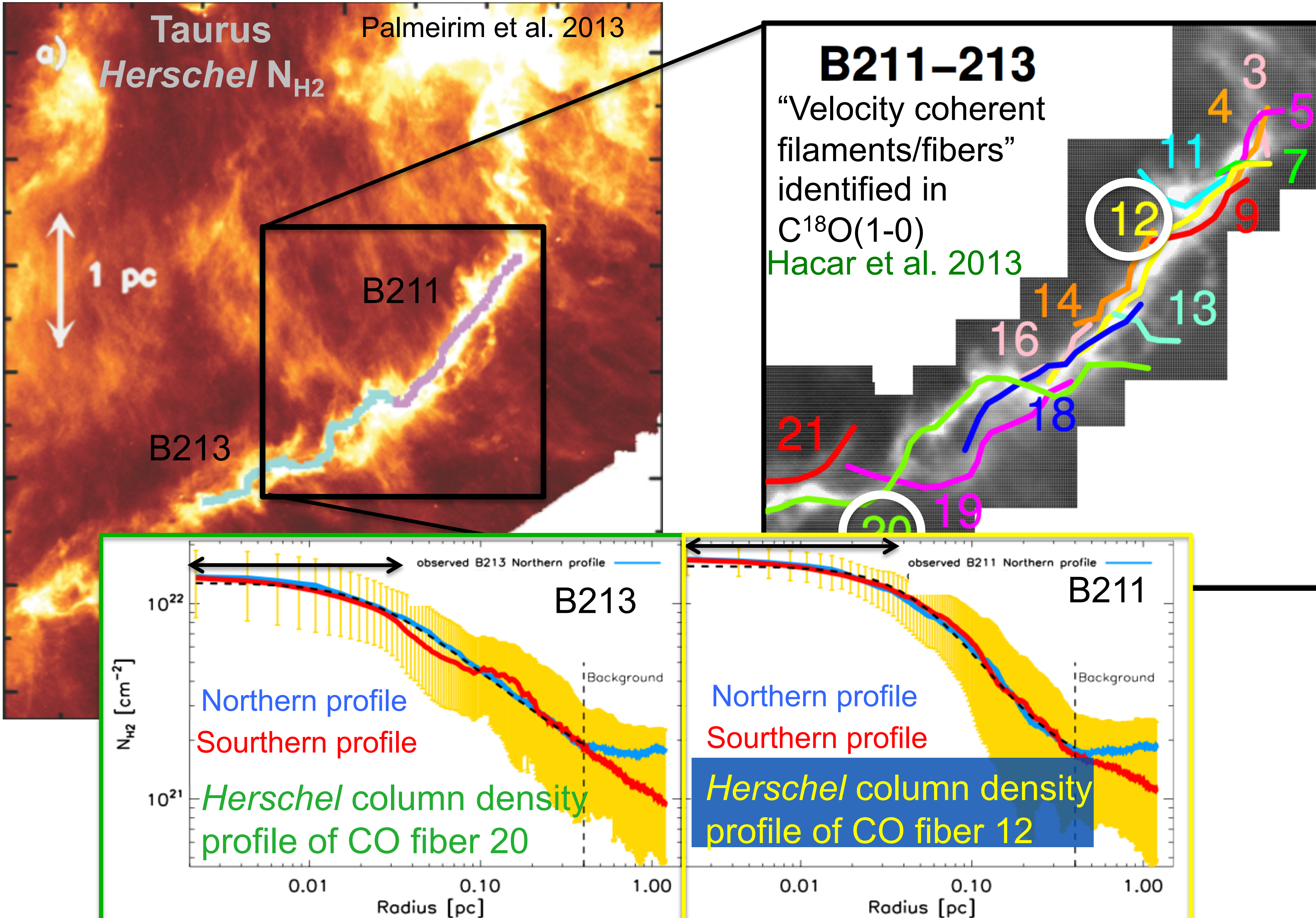

Nobeyama 45m observations of a filament on the verge of gravitational fragmentation in the Taurus molecular cloud

Investigating the interaction between the filament and its surroundings

Arzoumanian et al., in prep.

Herschel column density map

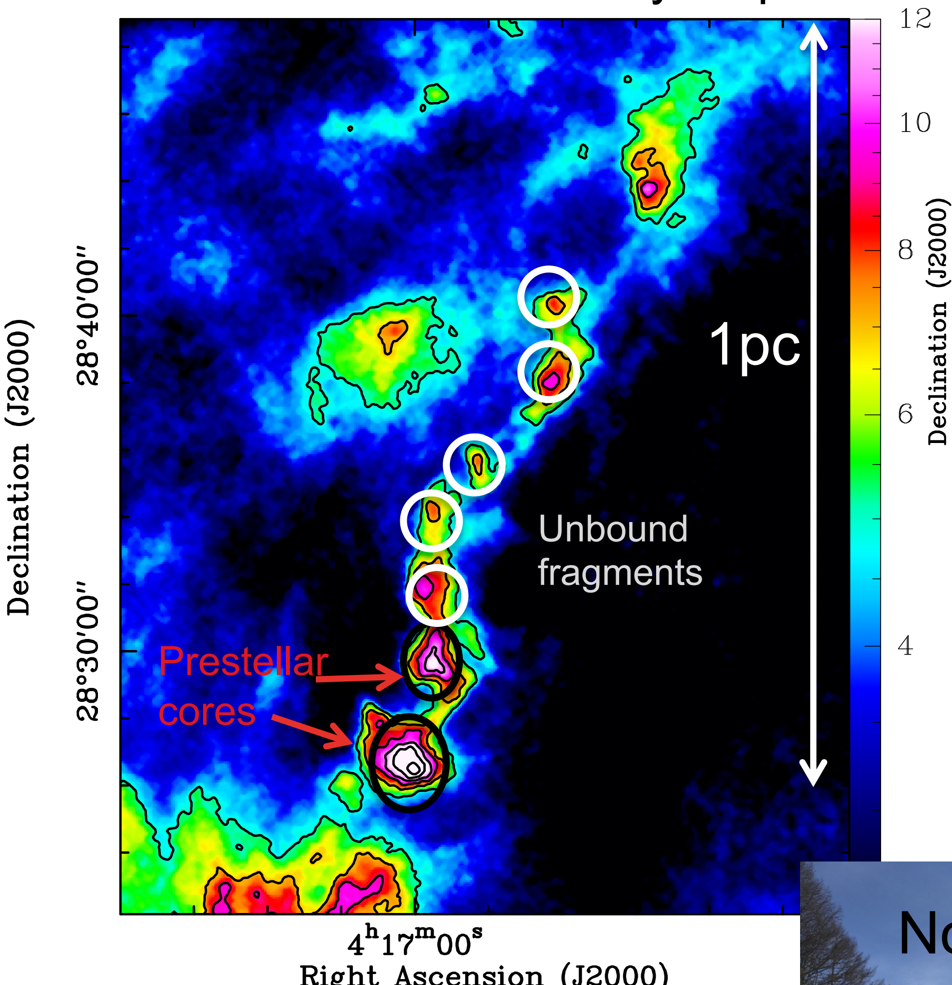

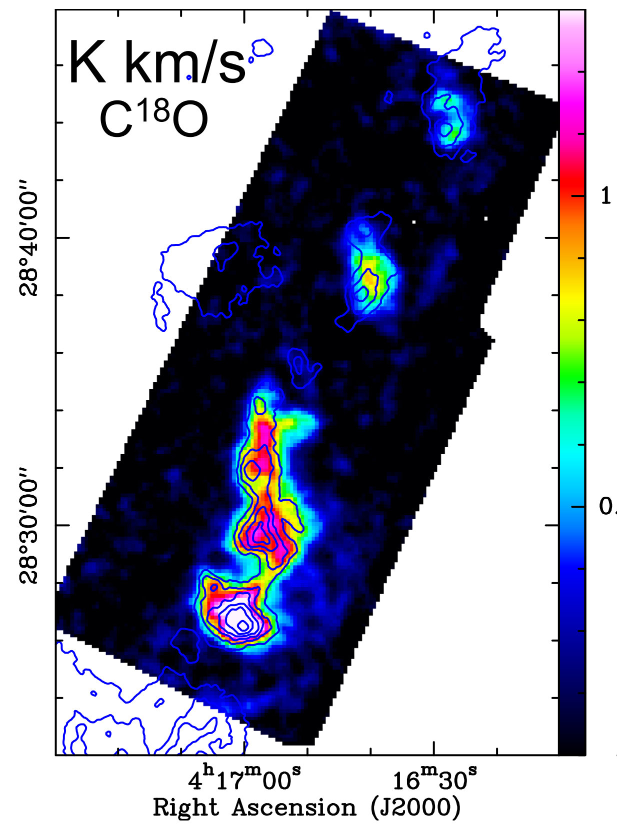

Map: Velocity [5-6km/s] integrated intensity of $C^{18}O(1-0)$

Contours:
Herschel N_{H2}
(5, 7, 9, 11, 13 x 10^{21} cm^{-2})

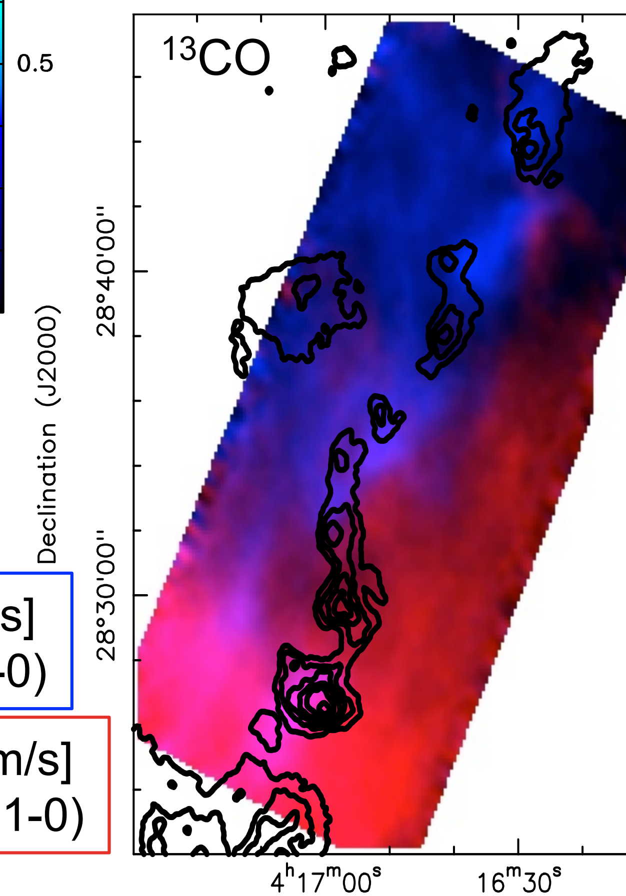

[4-5km/s] $^{13}CO(1-0)$

[6-7km/s] $^{13}CO(1-0)$

Doris Arzoumanian, MHD workshop, December 13, 2017, Kagoshima

Multiple velocity components are observed towards the filament

Arzoumanian et al., in prep.

Herschel column density map

PV cuts perpendicular to the filament and averaged along the crest

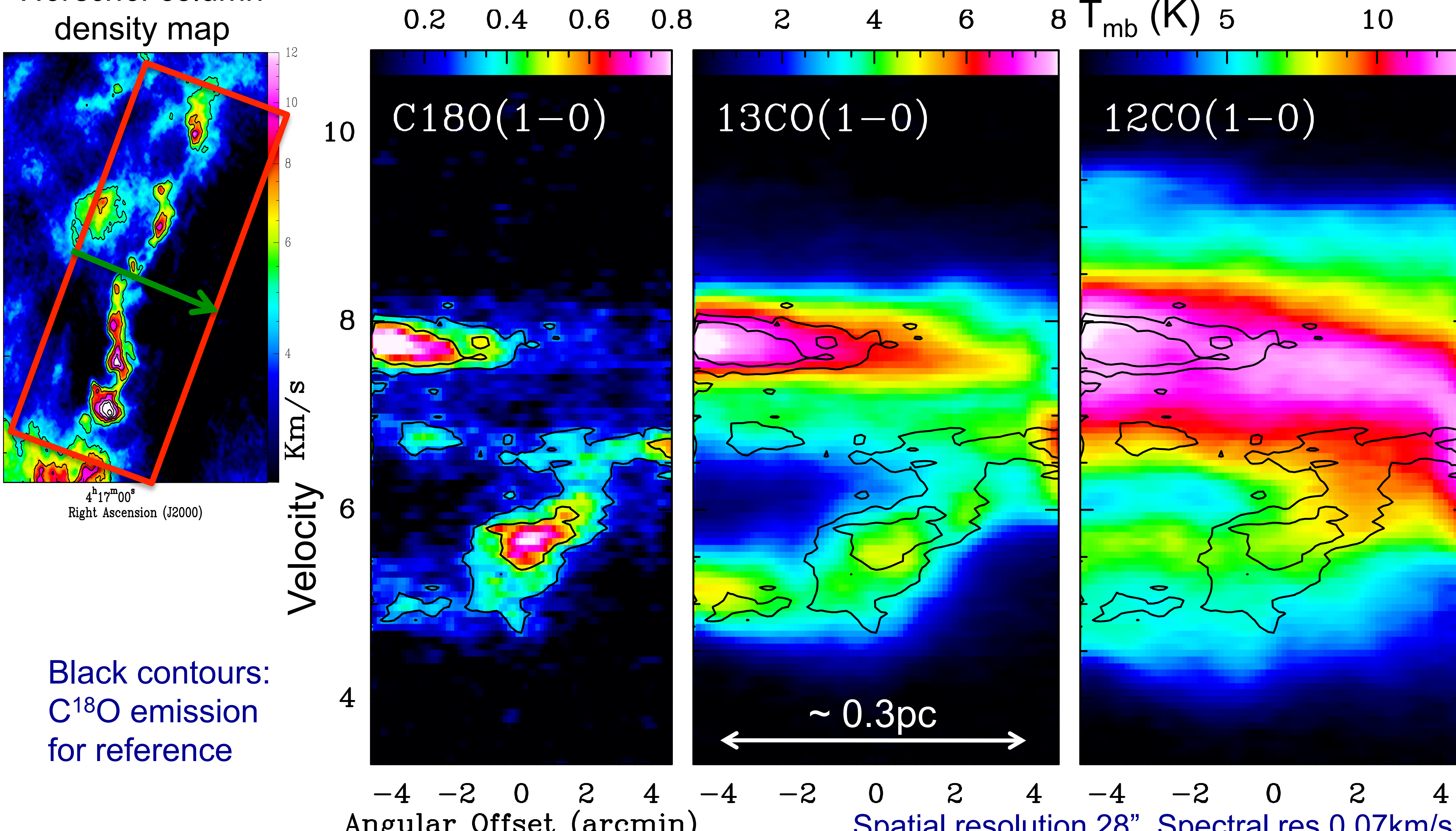

Black contours: $C^{18}O$ emission for reference

Spatial resolution 28", Spectral res 0.07km/s

Multiple velocity components are observed towards the filament, but they may correspond to extended structures surrounding the filament

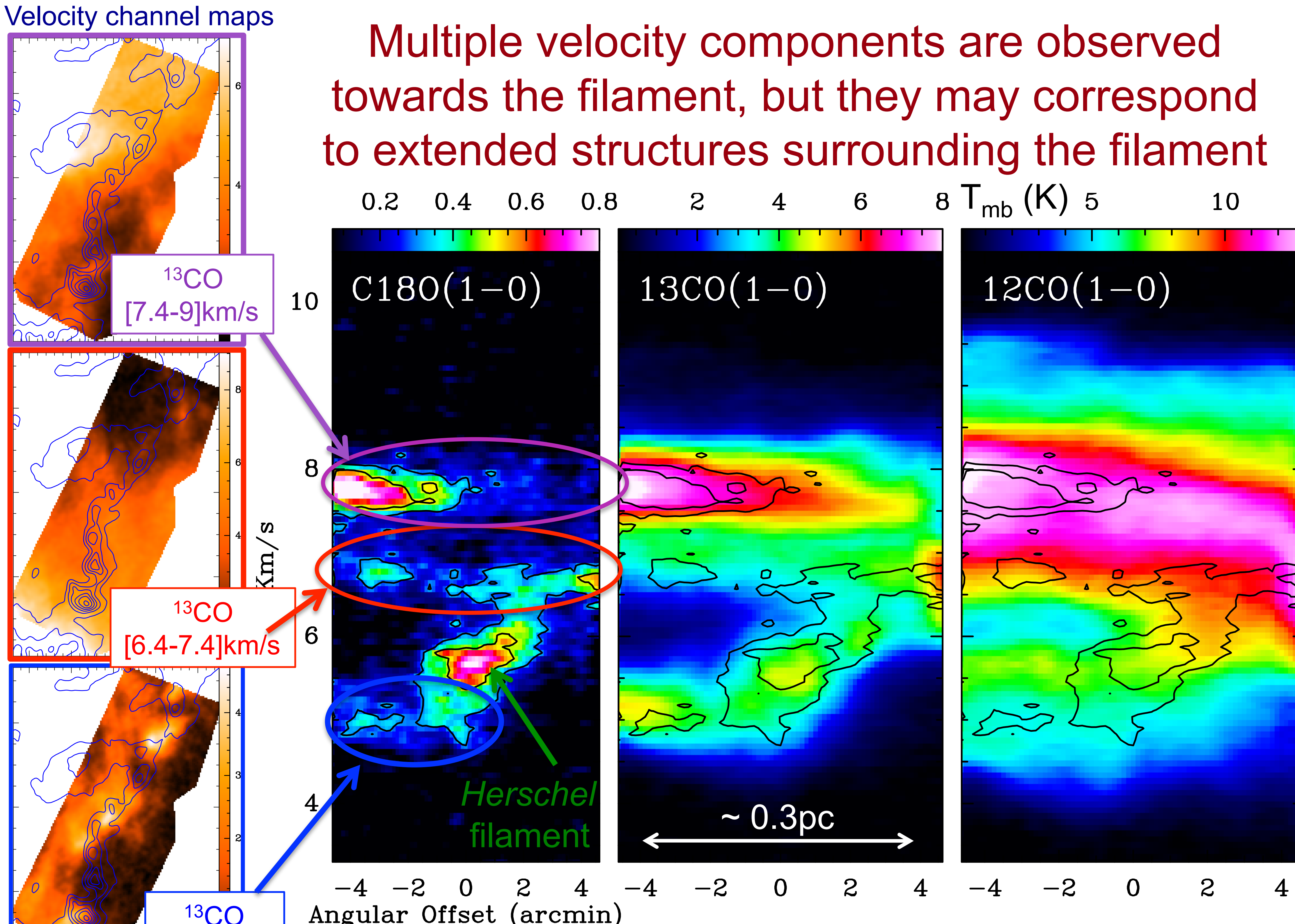

Doris Arzoumanian, MHD workshop, December 13, 2017, Kagoshima

Why thermal dust grain emission is linearly polarized and traces the ambiant B field structure?

• Linear polarization results from non-spherical dust grains

• Dust grains have paramagnetic property and are fast spinning, so they precess around the ambient magnetic field

→ These two properties make the dust polarized emission trace B field orientation
(e.g., Davis & Greenstein 1951, Vaillancourt 2007, Hoang, Lazarian, Andersson et al. 2014)

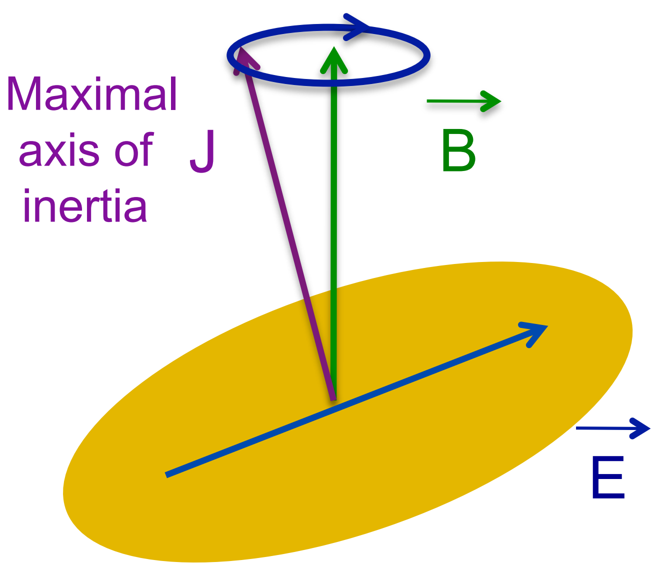

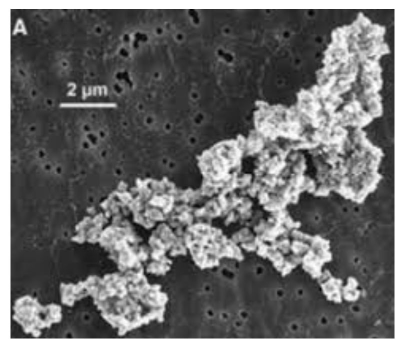

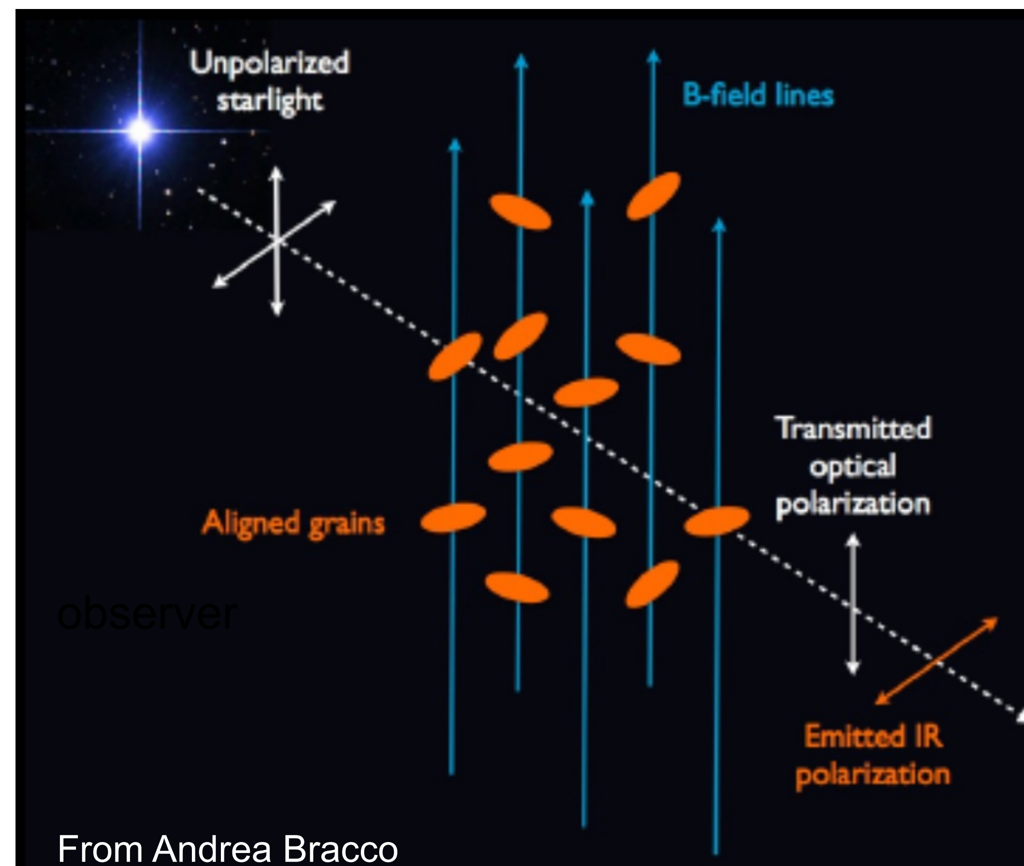

• Aspherical dust grains align their axis of maximal inertia with the local B-field orientation

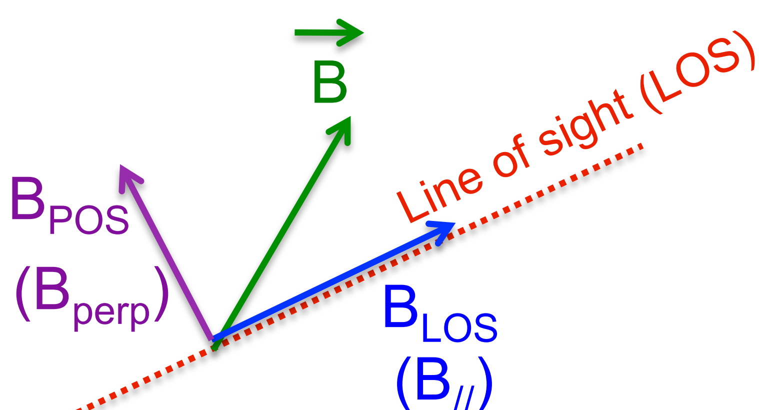

B orientation = pol. direction + 90°

The observed polarized emission depends on the structure of the magnetic field and the polarization efficiency of dust grains

Observed Stokes parameters

The imprint of the mean field geometry is present in *Q* and *U*, which are integrated quantities along the line of sight (LOS)

$$Q = \int p_0 \cos(2\psi)\cos^2(\gamma)\, dI$$

$$U = \int p_0 \sin(2\psi)\cos^2(\gamma)\, dI$$

(***I***: total intensity ~ column density)

Polarization properties of dust grains

Polarization angle, $\psi = 0.5 \arctan(-U, Q)$ + 90° orientation of B_{POS}

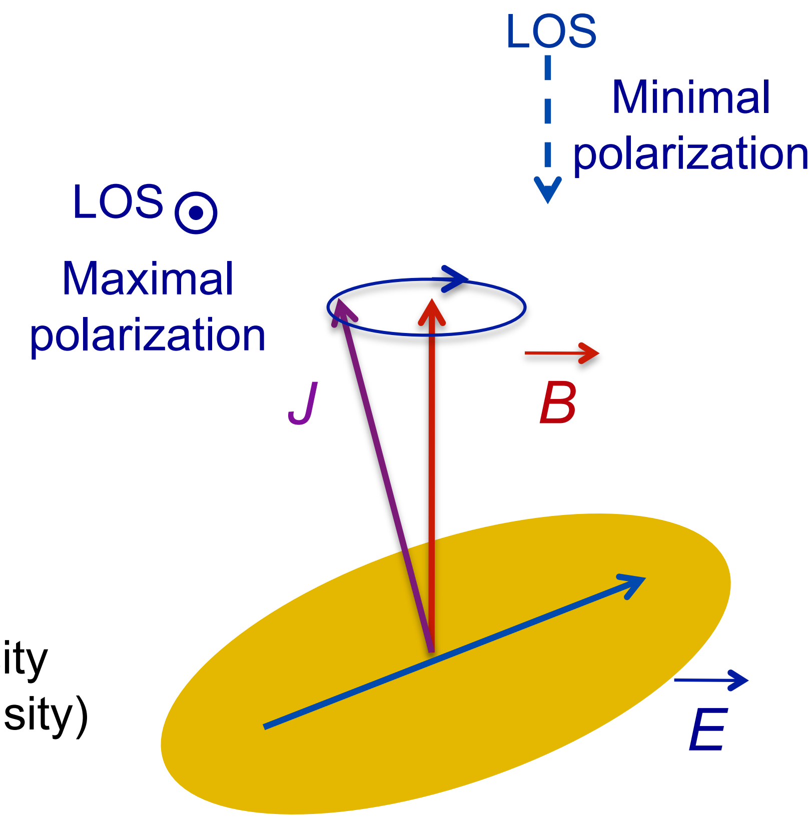

Linearly polarized thermal dust emission

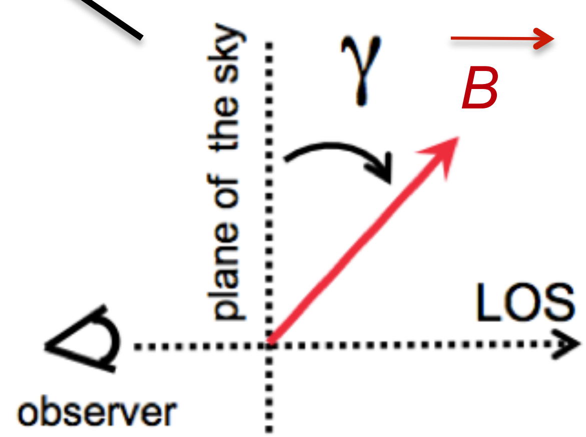

Polarization properties derived from the Stokes parameters

Polarized intensity

$$P = \sqrt{Q^2 + U^2}$$

Polarization fraction

$$p = P/I$$

The observed polarized emission depends on the structure of the magnetic field and the polarization efficiency of dust grains

$$p = \underbrace{p_{\text{dust}}}_{1}\ \underbrace{R}_{2}\ \underbrace{F}_{3}\ \underbrace{\cos^2\gamma}_{4}$$

Empirical parametrization of the observed polarization fraction

1) Dust properties: size, shape, composition (Voshchinnikov & Hirashita 2014)

2) Grain alignment efficiency with the local magnetic field (Goodman 1992, Whittet et al 2008, Hoang & Lazarian 2014)

3) Depolarization from
2 (or more) layers along the LOS

$F=P/(P_1+P_2)$

$$P^2 = P_1^2 + P_2^2 + 2P_1P_2\cos 2\Delta\psi$$

(Jones et al. 1992, 2015, Myers & Goodman 1991, *Planck* 2015 XX, 2016 XXXIII)

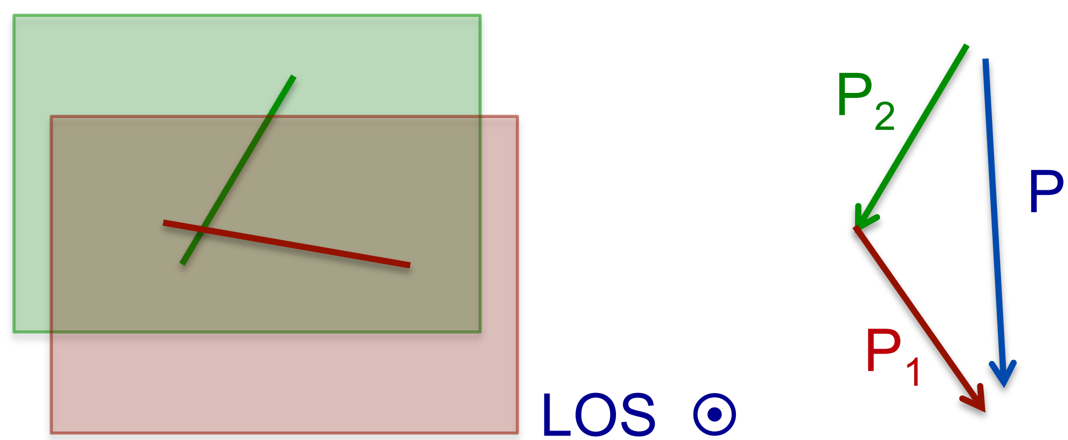

4) Field geometry
$\cos^2\gamma$

(Planck 2015 XX, 2016 XXXIII)

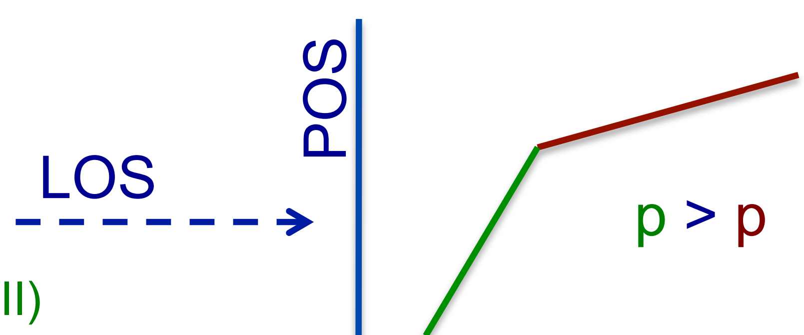

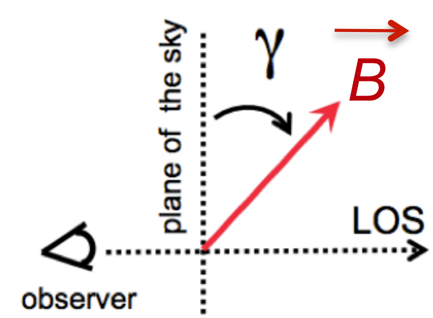

Doris Arzoumanian, MHD workshop, December 13, 2017, Kagoshima

What are the limitations in using thermal dust polarized emission to trace the mangetic field structure in the ISM?

$$p = p_{\text{dust}} \; R \, F \, \cos^2 \gamma$$

1 2 3 4

Dust grain properties

Magnetic field structure

Empirical parametrization of the observed polarization fraction

Degeneracy between all these factors: Details modelling of grain properties and understanding of the B field structure is important

Whole sky *Planck* dust polarization results on the dispersion of polarization fraction

Polarization fraction vs. gas column density

Planck 2015 XIX

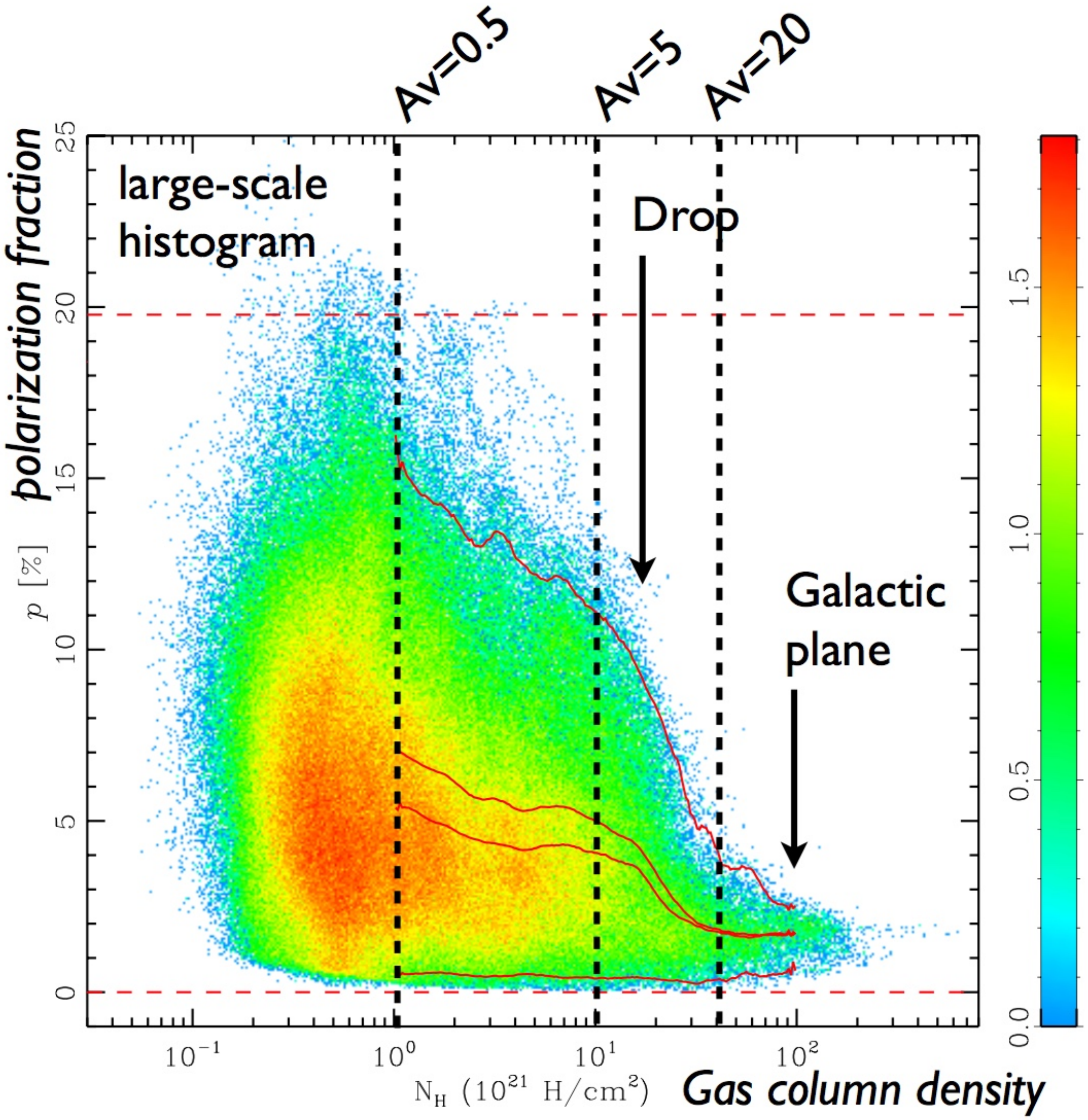

Total intensity + $\boldsymbol{B}_{POS}$ orientation

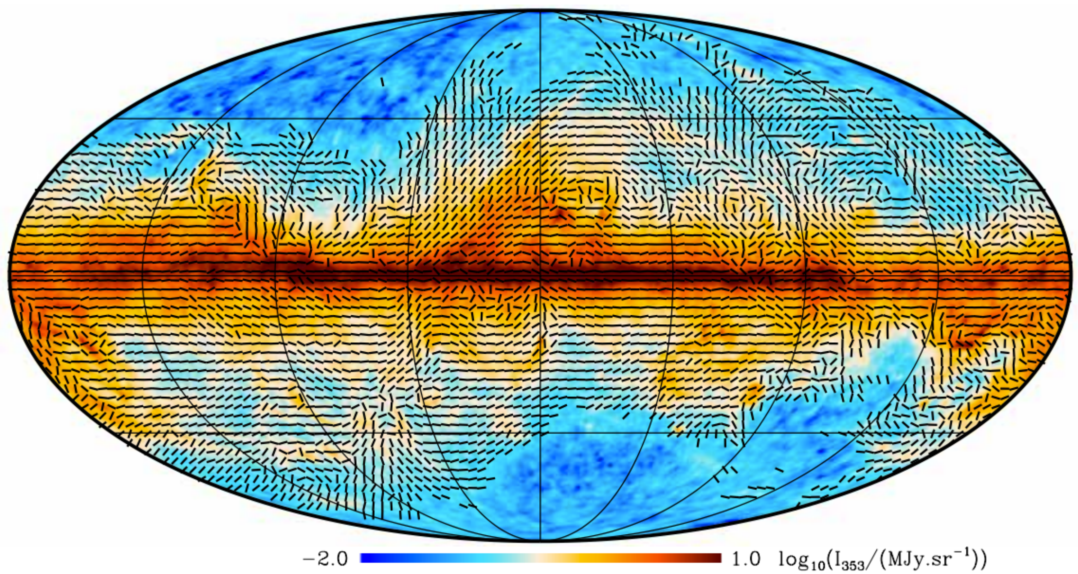

Polarization fraction

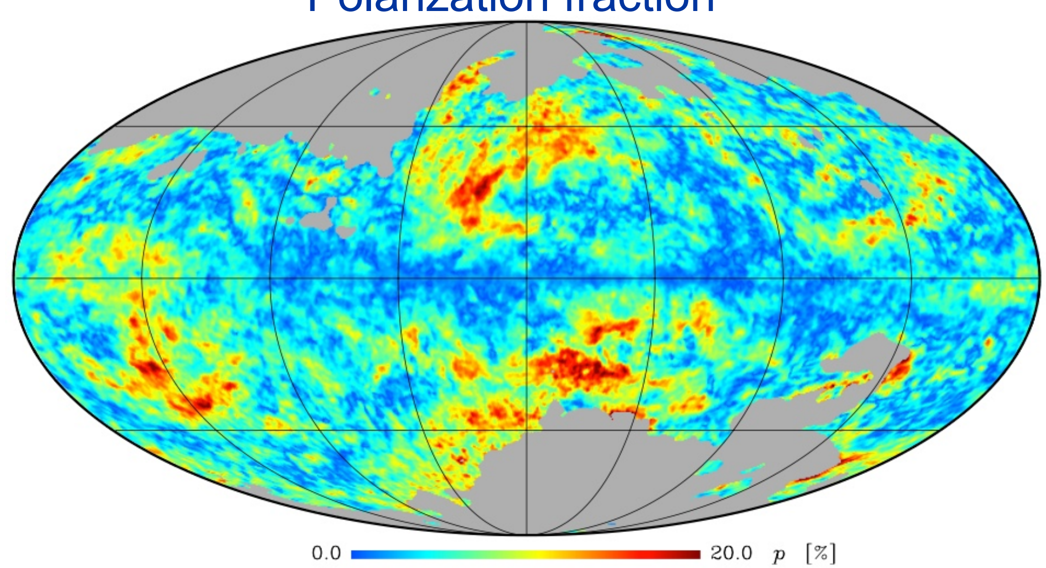

- Large scatter in p for each N_H bin
- Drop of p at large N_H values

Dust polarization observations with JCMT/SCUBA2-POL2
Variations of the polarization angle and the polarization fraction for high column density regions (> 10Av)

BISTRO observations towards Oph-A

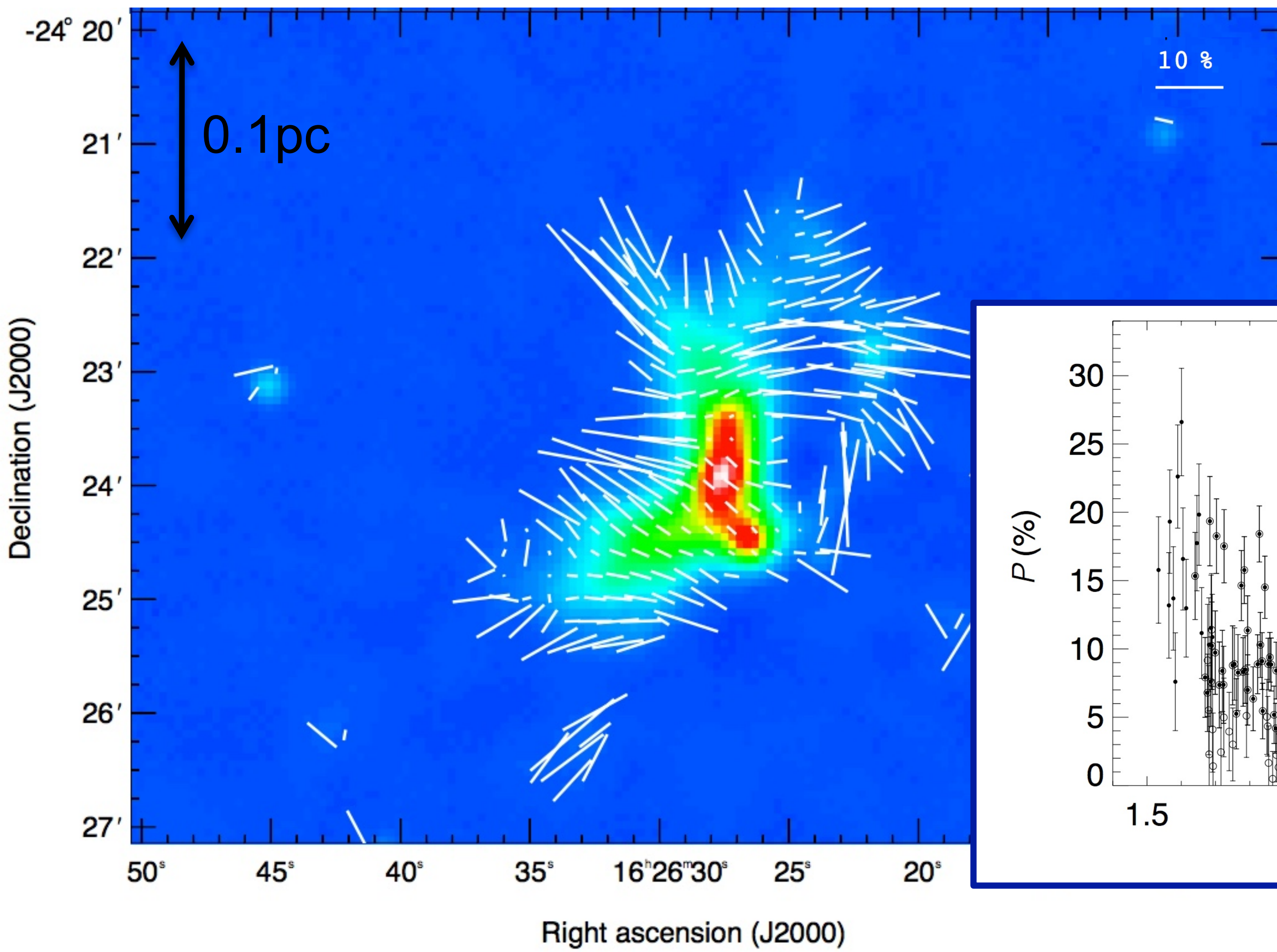

Kwon et al., submitted

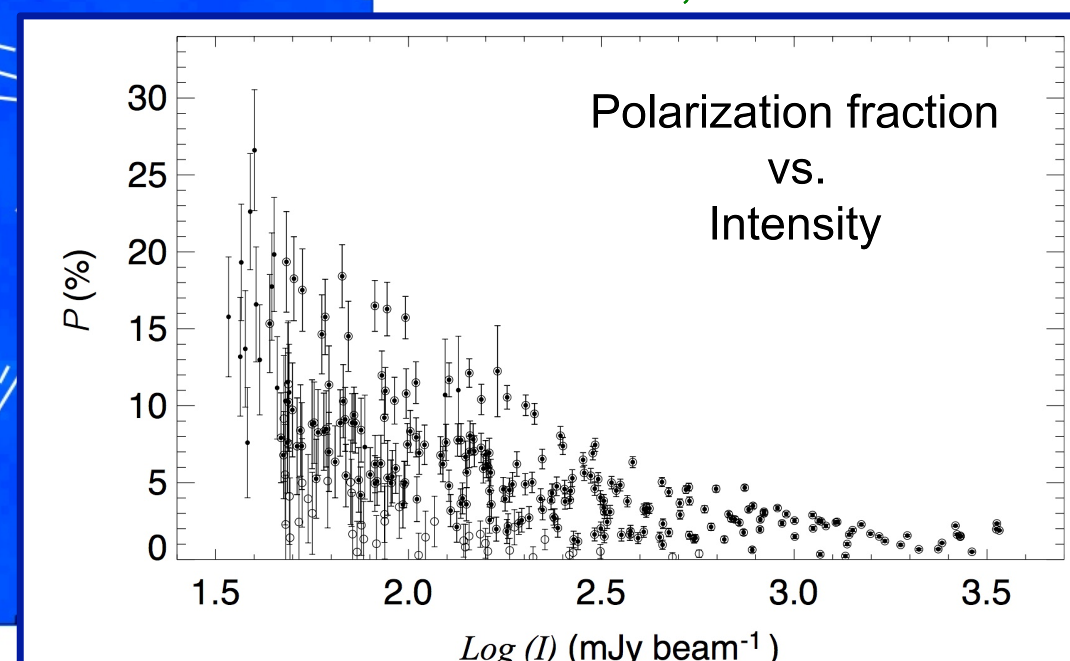

Image: SCUBA2 at 850μm (14.1”)

Segments: POS B-field from POL2 at 850μm (14.1”)

Understanding the observed polarization properties: Hint from numerical simulations of MHD turbulence

Philosophy:

-Producing I, Q, U maps from MHD simulation
-Computing the observable quantities, e.g., p
-Assuming uniform grain alignment and dust grain properties
-Varying the line of sight integration to mimic variation of orientation of the magnetic field with respect to the line of sight

$$p = p_{\text{dust}} \, R \, F \, \cos^2 \gamma$$

Uniform
Dust properties

Magnetic field
structure

Colliding flow turbulent MHD simulation of molecular cloud formation

Reprojecting Bx,By,Bz of the simulation into psi and gamma

Computing I,Q, and U maps from the simulation cube

$$I = \int S_\nu e^{-\tau_\nu} \left[1 - p_0 \left(\cos^2\gamma - \frac{2}{3}\right)\right] d\tau_\nu;$$

$$Q = \int p_0 \, S_\nu e^{-\tau_\nu} \cos(2\phi) \cos^2\gamma \, d\tau_\nu;$$

$$U = \int p_0 \, S_\nu e^{-\tau_\nu} \sin(2\phi) \cos^2\gamma \, d\tau_\nu.$$

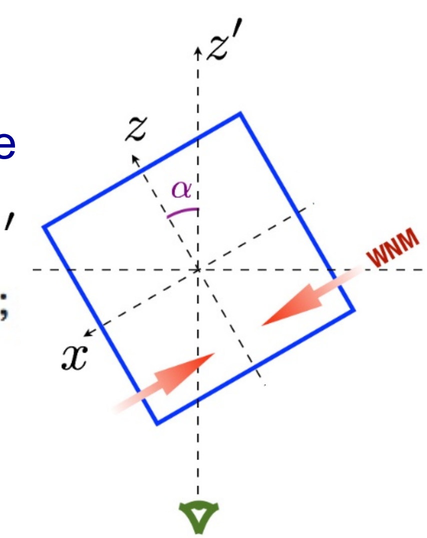

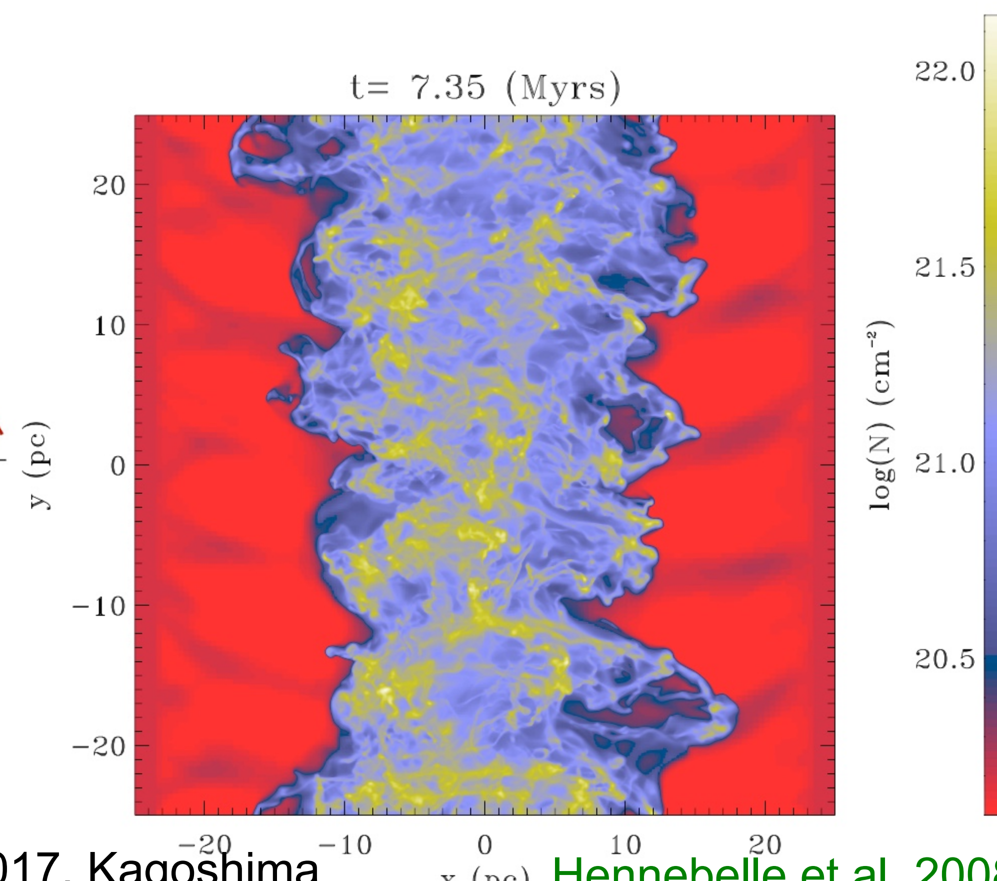

Hennebelle et al. 2008

Understanding the observed polarization properties: Hint from numerical simulations of MHD turbulence

Results:

-Observations are well produced by numerical simulations up to a ~10Av, with non variation of dust grain properties

-Depolarization along the LOS and the orientation of the mean magnetic field with respect to the LOS play a role in reproducing the observations

$$p = p_{dust} \, R \, F \, \cos^2 \gamma$$

Uniform
Dust properties

Magnetic field
structure

Polarization fraction vs column density

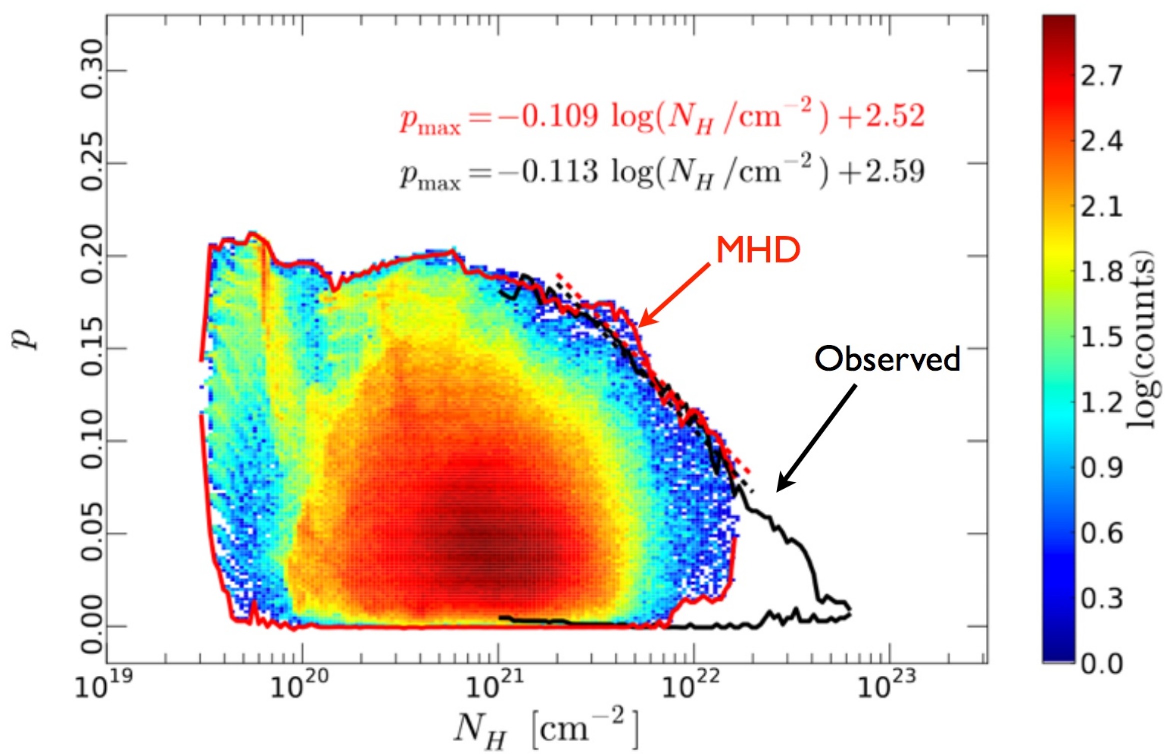

Simulations reproduce well the decrease of p_{max} with N_H in the range 10^{21} to 2×10^{22} cm^{-2}

Colliding flow turbulent MHD simulation of molecular cloud formation

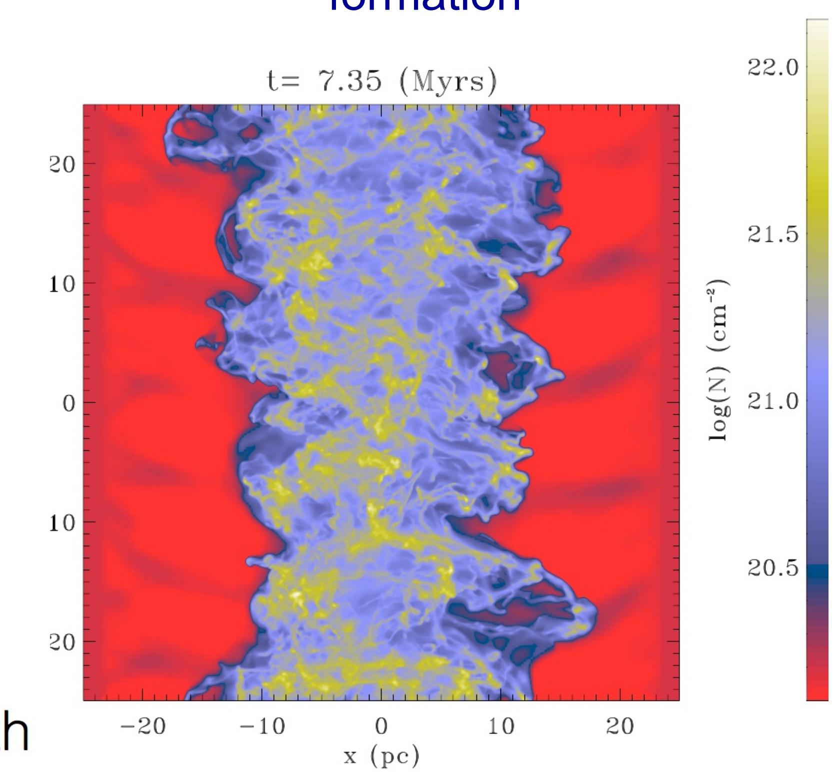

Hennebelle et al. 2008

Understanding the observed polarization properties: modelling the distribution of p and psi of the Galactic pole

Planck XLIV 2016, Andrea Bracco

Phenomenological model:

- Modeling the dust polarization observations towards the Galactic pole
- Characterizing the ordered (Lon^0 and Lat^0) and turbulent (random) components of the Galactic magnetic field in the solar neighbourhood
- The line of sight depolarization is modeled by summing the emission over a number of layers with independent realizations of turbulence (B_{turb})
- Assuming uniform grain alignment and dust grain properties

$$\vec{B} = \vec{B}_0 + \vec{B}_{turb} \qquad (< \vec{B}_{\mathrm{turb}} >= 0)$$

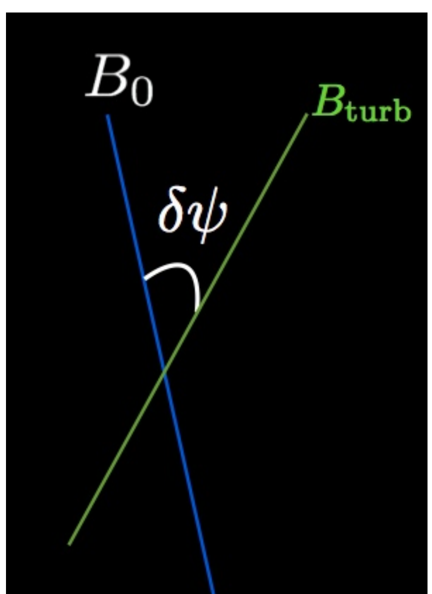

Layers with independent turbulence along the line of sight

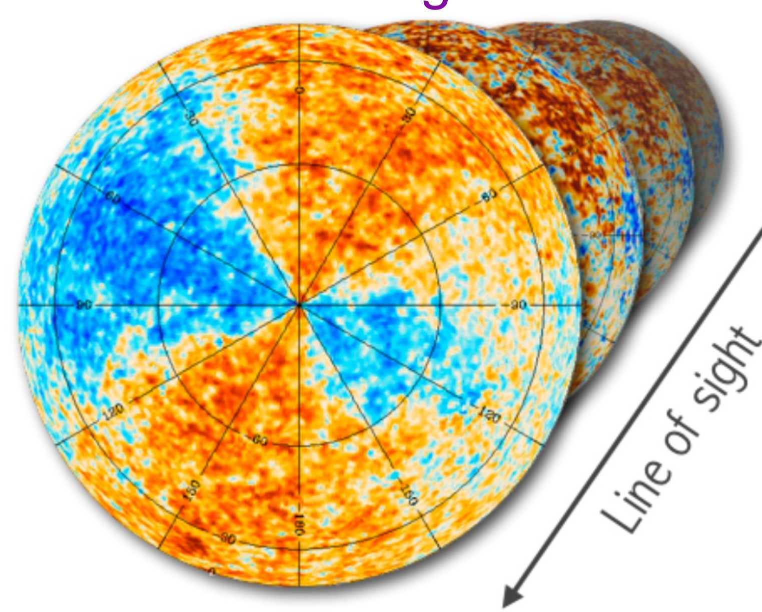

Understanding the observed polarization properties: modelling the distribution of p and psi of the Galactic pole

Results: The Galactic mean field

-The observations can be modeled with $(Lon^0, Lat^0)=(80^o, 0^o)$, a uniform direction of the Galactic magnetic field.

same values are also infered from starlight polarization (Heiles 1996)

Stokes parameters centered on the south Galactic pole

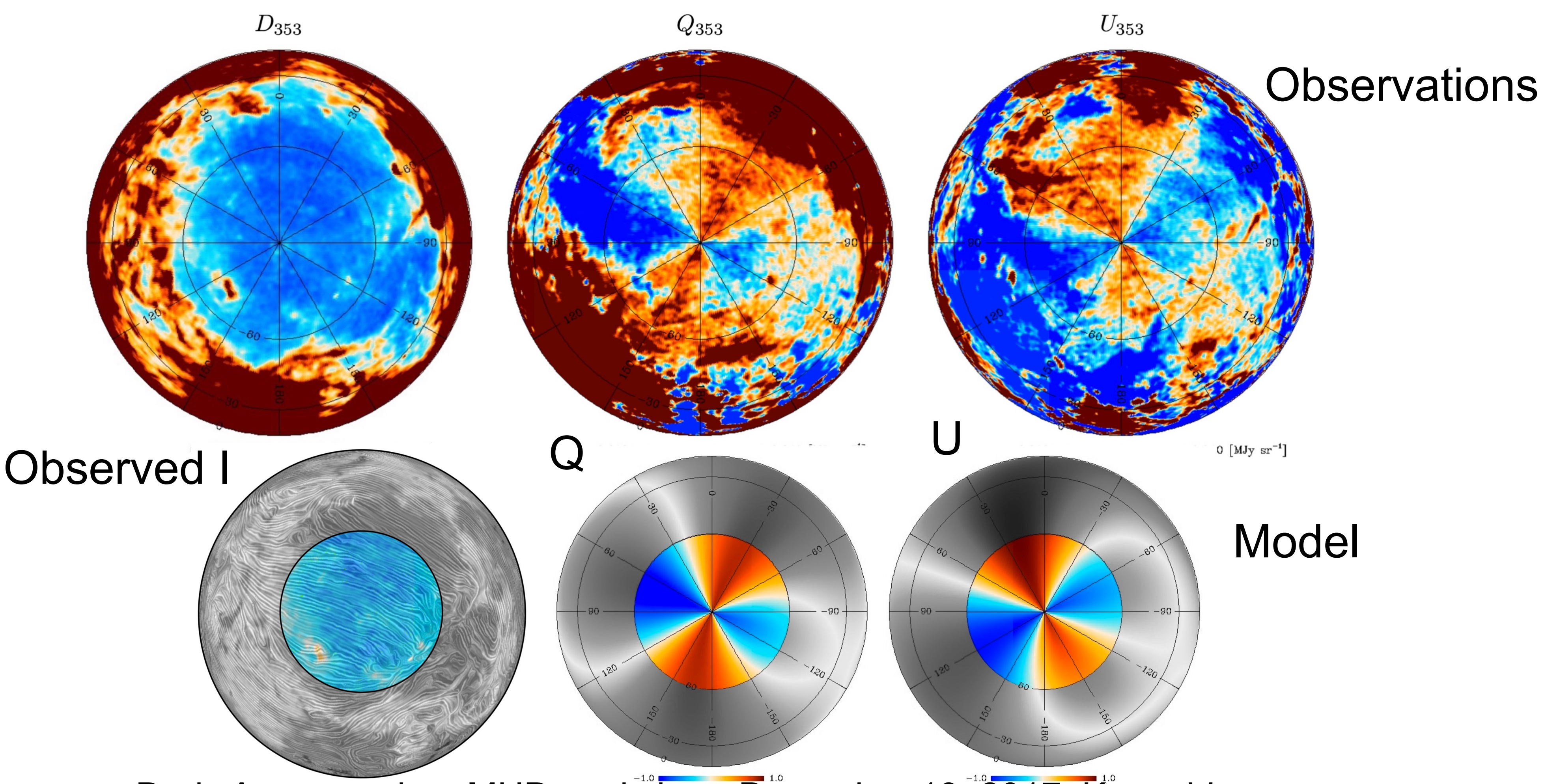

Understanding the observed polarization properties: modelling the distribution of p and psi of the Galactic pole

Results: Distributions of polarization angle and fraction with one layer model

- One layer with an ordered field B_0 and a turbulent component B_{turb}
- Uniforme dust grain intrinsic polarization

$$\vec{B} = \vec{B}_0 + \vec{B}_{turb} \qquad (<\vec{B}_{\mathrm{turb}}>=0)$$

→ The wide distribution of the polarization fraction cannot be reproduced with a single layer model

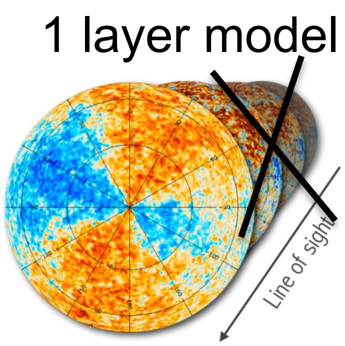

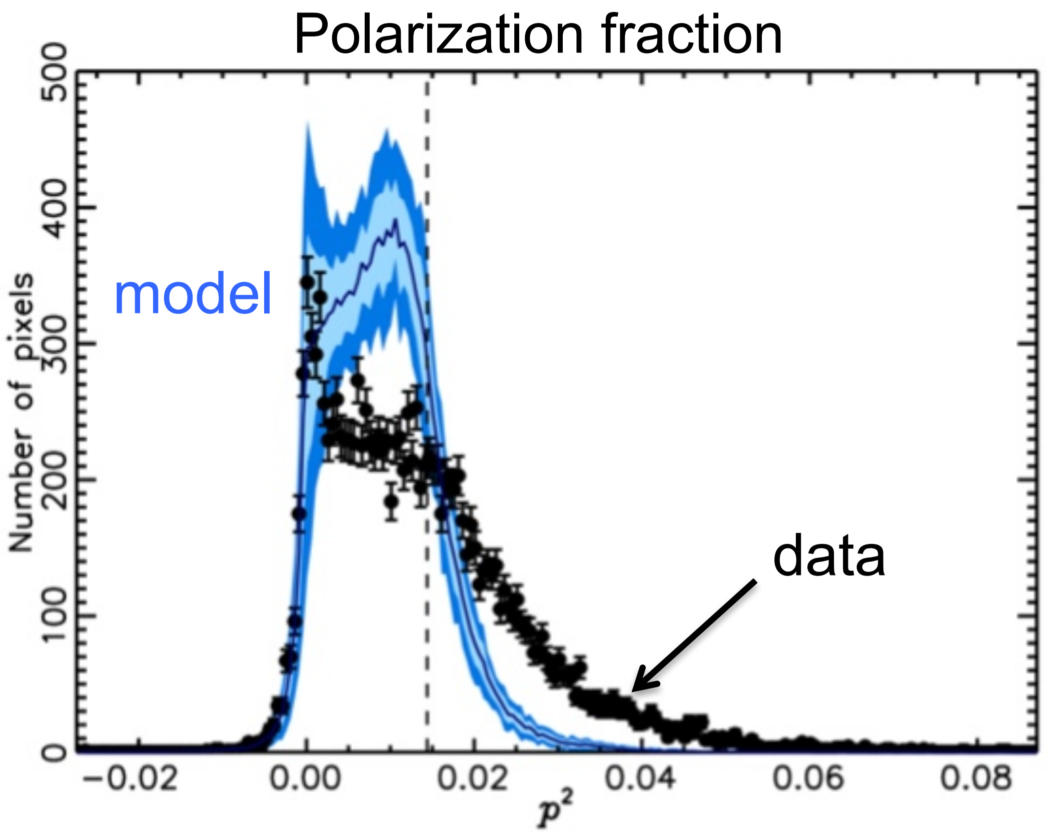

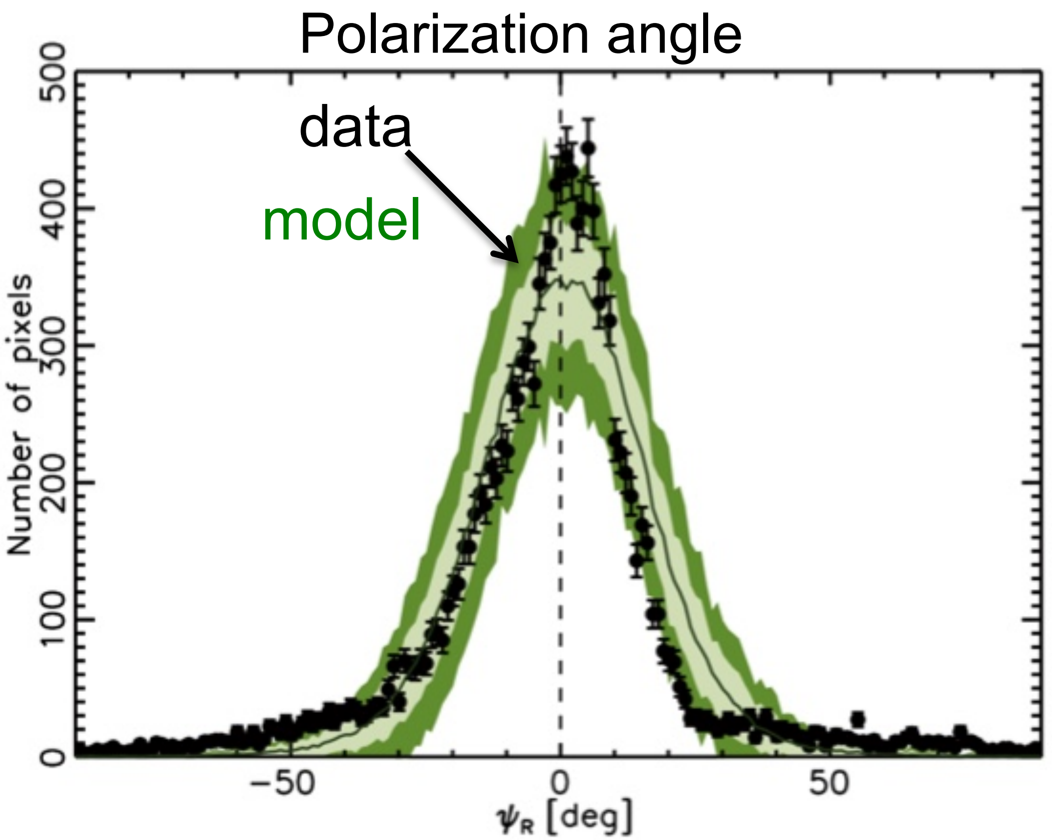

Understanding the observed polarization properties: modelling the distribution of p and psi of the Galactic pole

Results: Distributions of polarization angle and fraction with multiple layer model

→The observations are well reproduced with

- Ratio of B_{turb}/ B_0 ~0.8
- Uniforme dust grain intrinsic polarization p_{max}=26%
- When integrating over 7 layers along the line of sight

Model with multiple layers along the line of sight

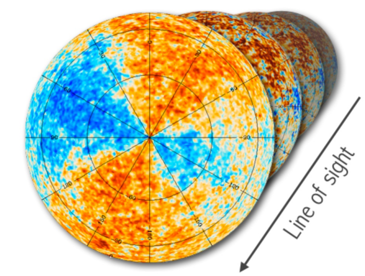

(The number of layers along the line of sight can also be understood in terms of the exponent of the power spectrum of B_{turb} along the line of sight)

Polarization fraction

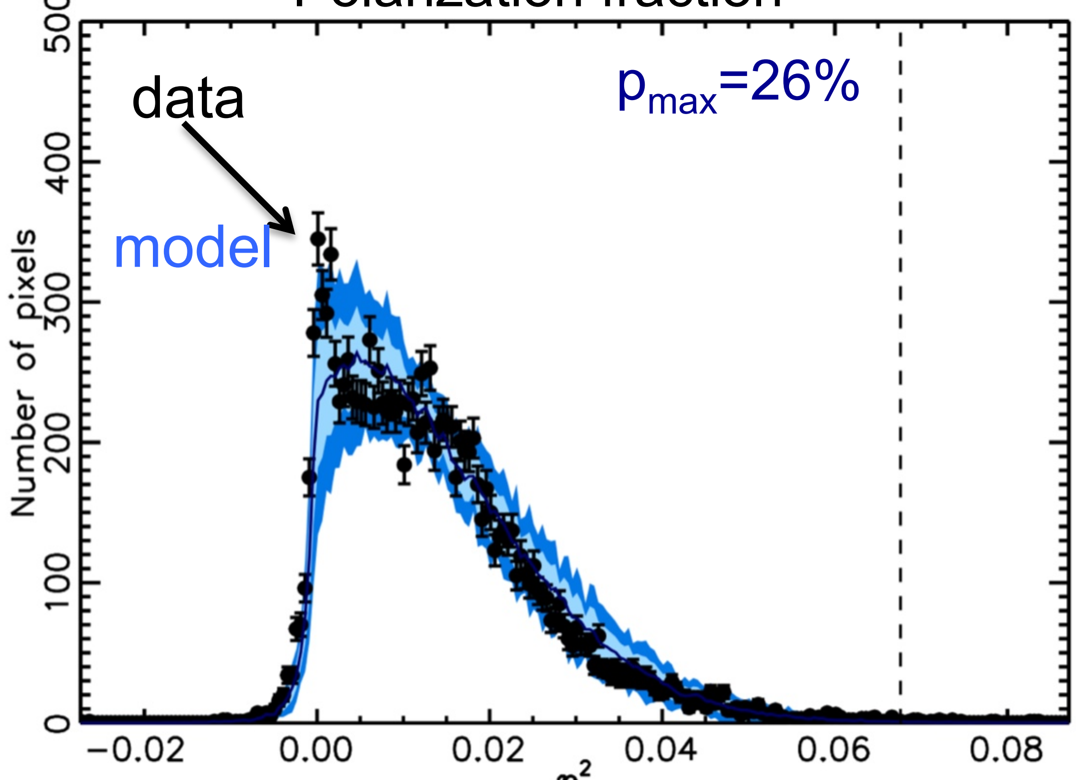

Polarization angle

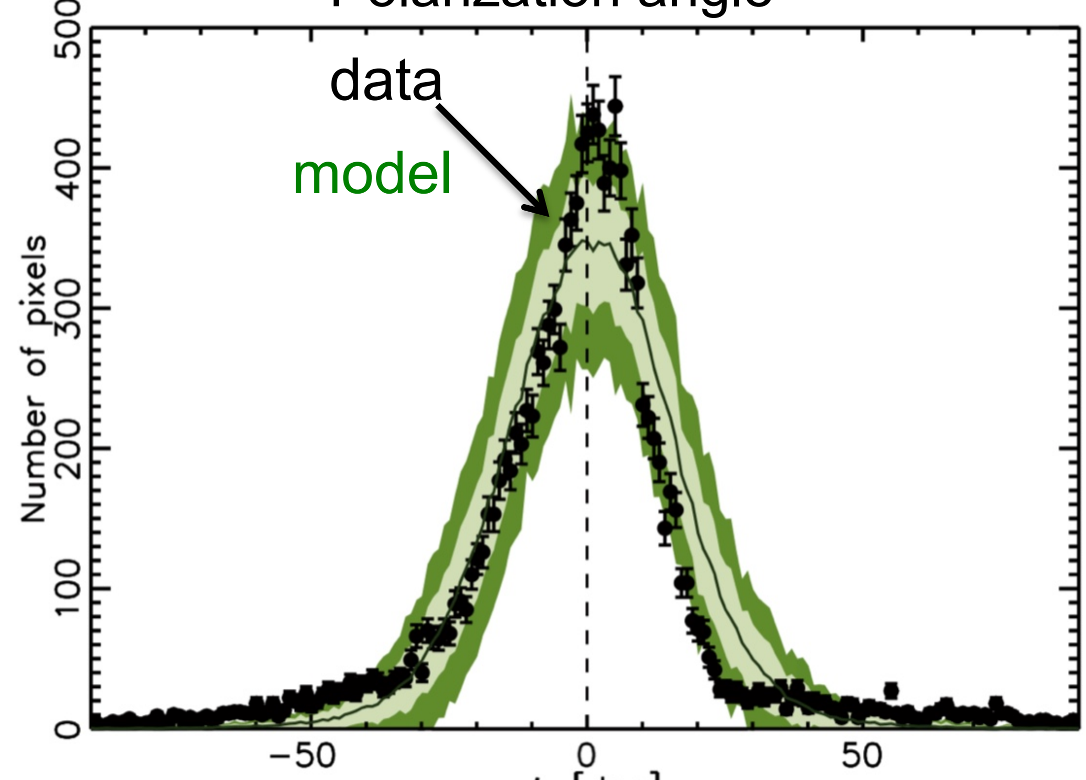

Tow layers along the line of sight: the filament and its background

Mean radial profiles of the Stokes parameters and fit of the background

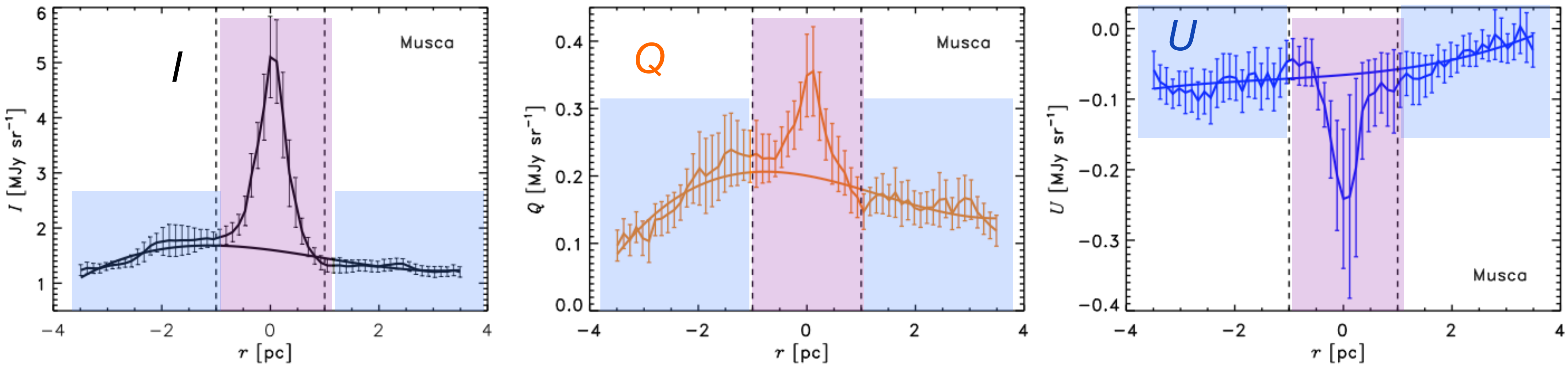

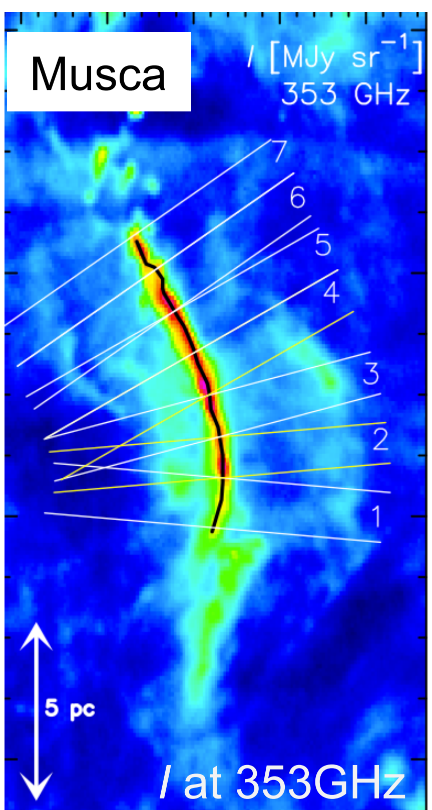

Two layer model to estimate the contribution of the filament to the total observed emission

$$I_{tot} = I_{bg} + I_{fil}$$

$$U_{tot} = U_{bg} + U_{fil}$$

$$Q_{tot} = Q_{bg} + Q_{fil}$$

$$P = \sqrt{Q^2 + U^2} \qquad p = P/I$$

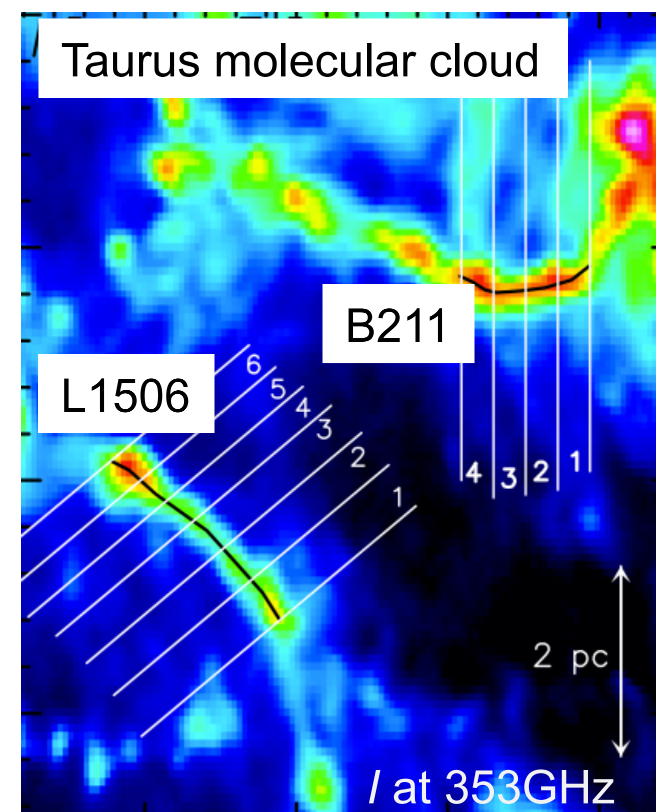

$\psi = 0.5 \arctan(-U, Q)$ $+90^{o}$ = $\boldsymbol{B}_{POS}$ angle

Variation of the polarization fraction (p) from the parent cloud to the filament

- The observed polarization fraction (p) towards the filaments show a decrease with respect to p in the background.
- For Musca and B211 the intrinsic p in the filaments is smaller than what is observed without component separation, for L1506 p in the filament is larger than the observed value (filament + background)

Polarization fraction (%) across the filaments (at 5')

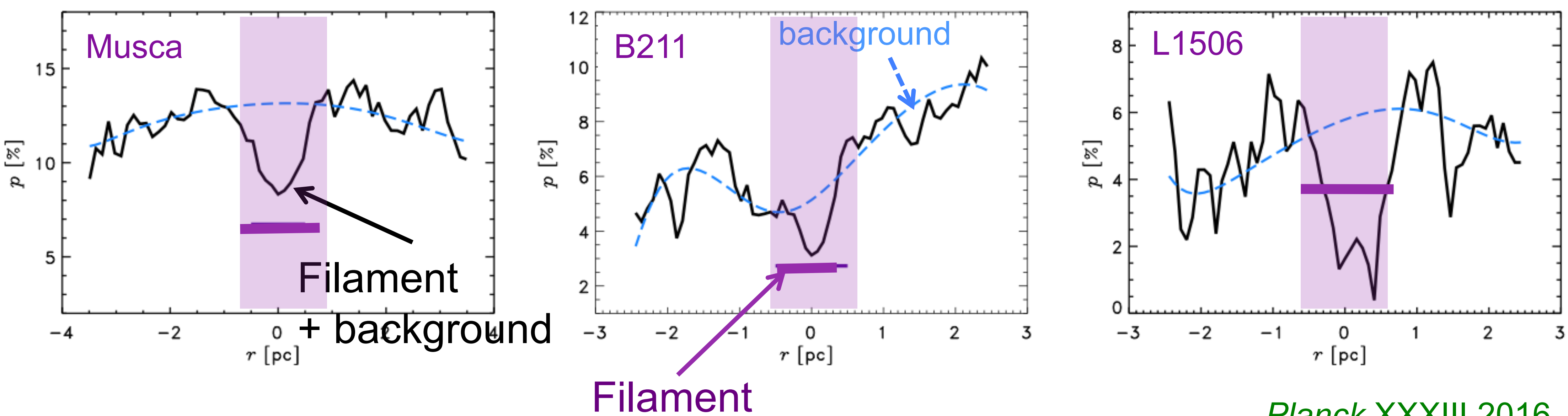

Planck XXXIII 2016

Polarization fraction

$$p = P/I$$

I: total intensity

Polarized intensity

$$P = \sqrt{Q^2 + U^2}$$

Depolarization from LOS integration

Superposition, along the LOS, of 2 layers with different $B_{\rm POS}$ angles (filament + background)

$$p = p_{\rm dust}\, R\, F \cos^2\gamma$$

$$F = \frac{P}{P_{\rm fil} + P_{\rm bg}}$$

$$P^2 = P_1^2 + P_2^2 + 2P_1 P_2 \cos 2\Delta\psi$$

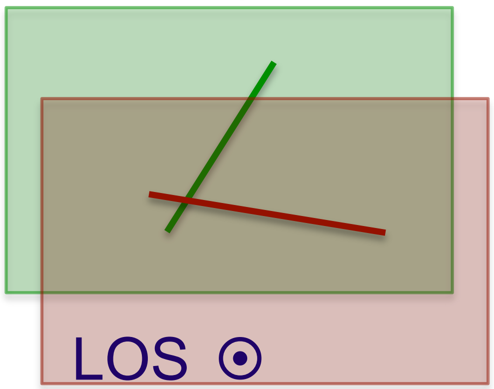

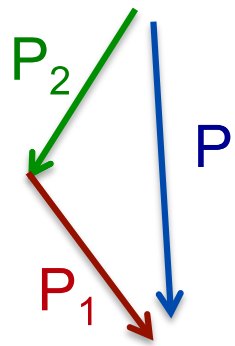

Planck XXXIII 2016

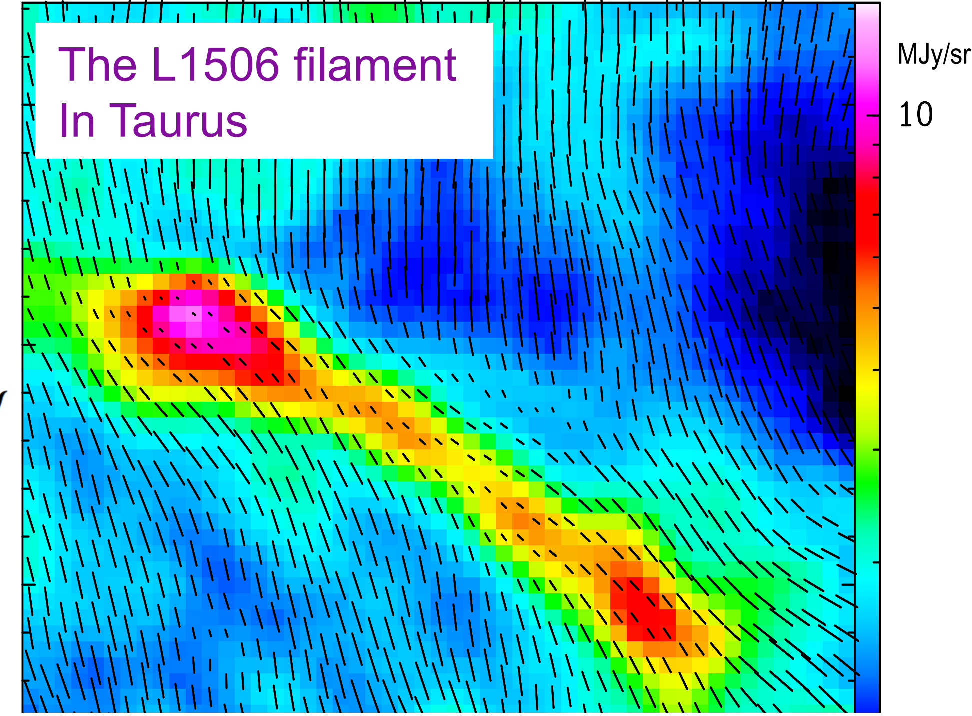

Planck total intensity at 353GHz (850μm) in MJy/sr
Segments: $\boldsymbol{B}_{\rm POS}$ length ~ polarization fraction
(10' resolution)

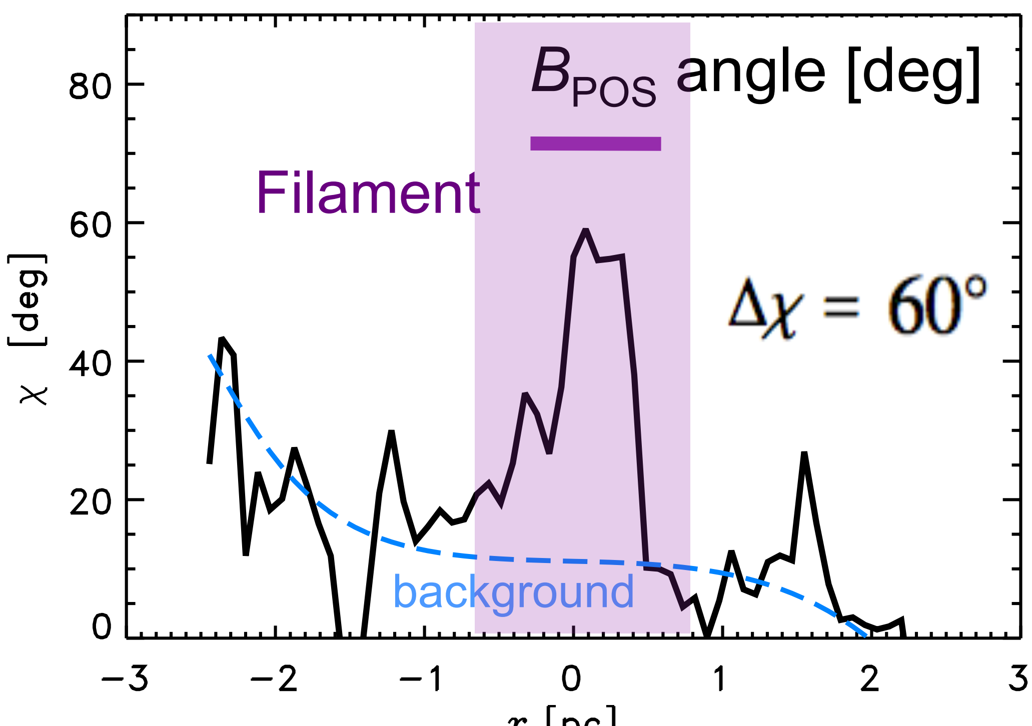

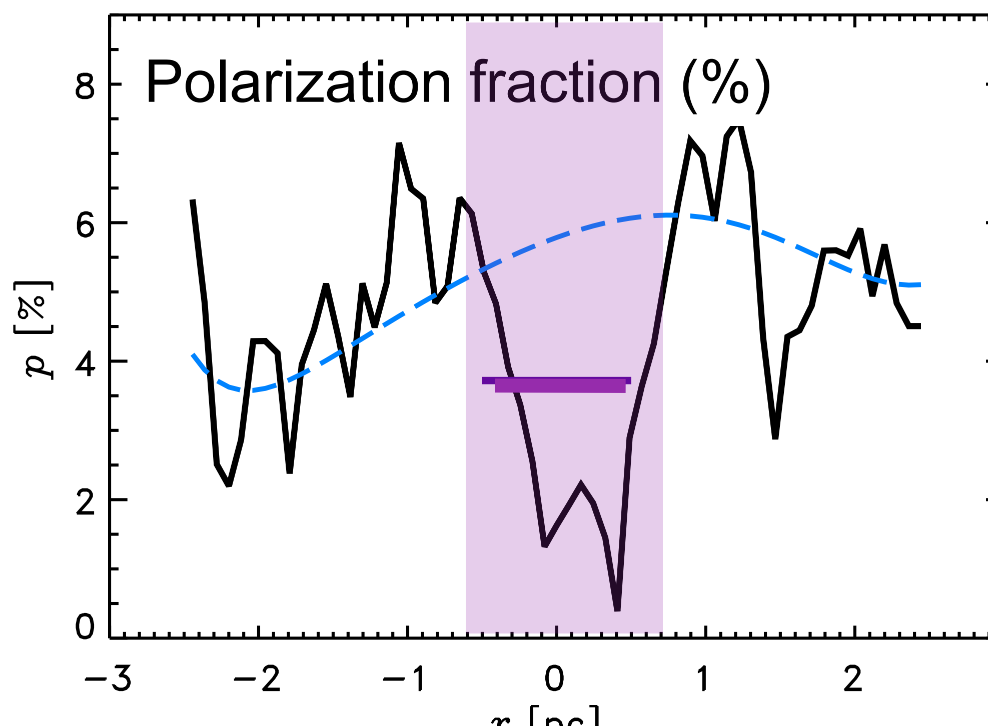

Variations of the polarization angle and the polarization fraction: Insight on the 3D magnetic field structure in the filaments?

Role of the geometry of the magnetic field in the observed 0.1 pc width of filaments?

Increase of the magnetic pressure due to the compression of the magnetic field lines: may prevent the further collapse of the filament?

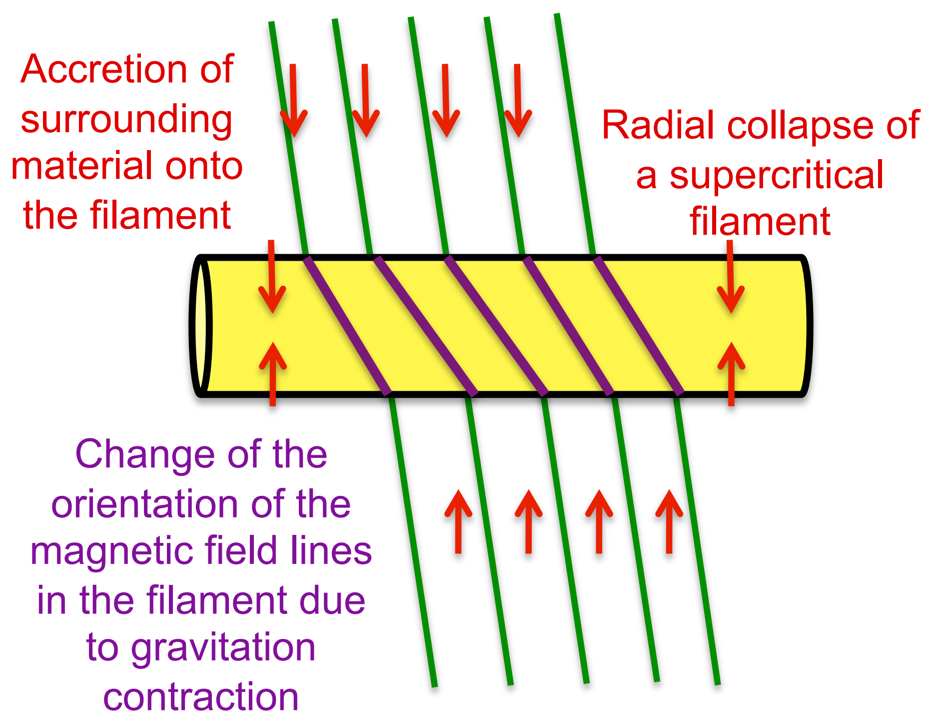

Planck XXXIII 2016 (arXiv:1411.2271)

The L1506 filament in the Taurus molecular cloud

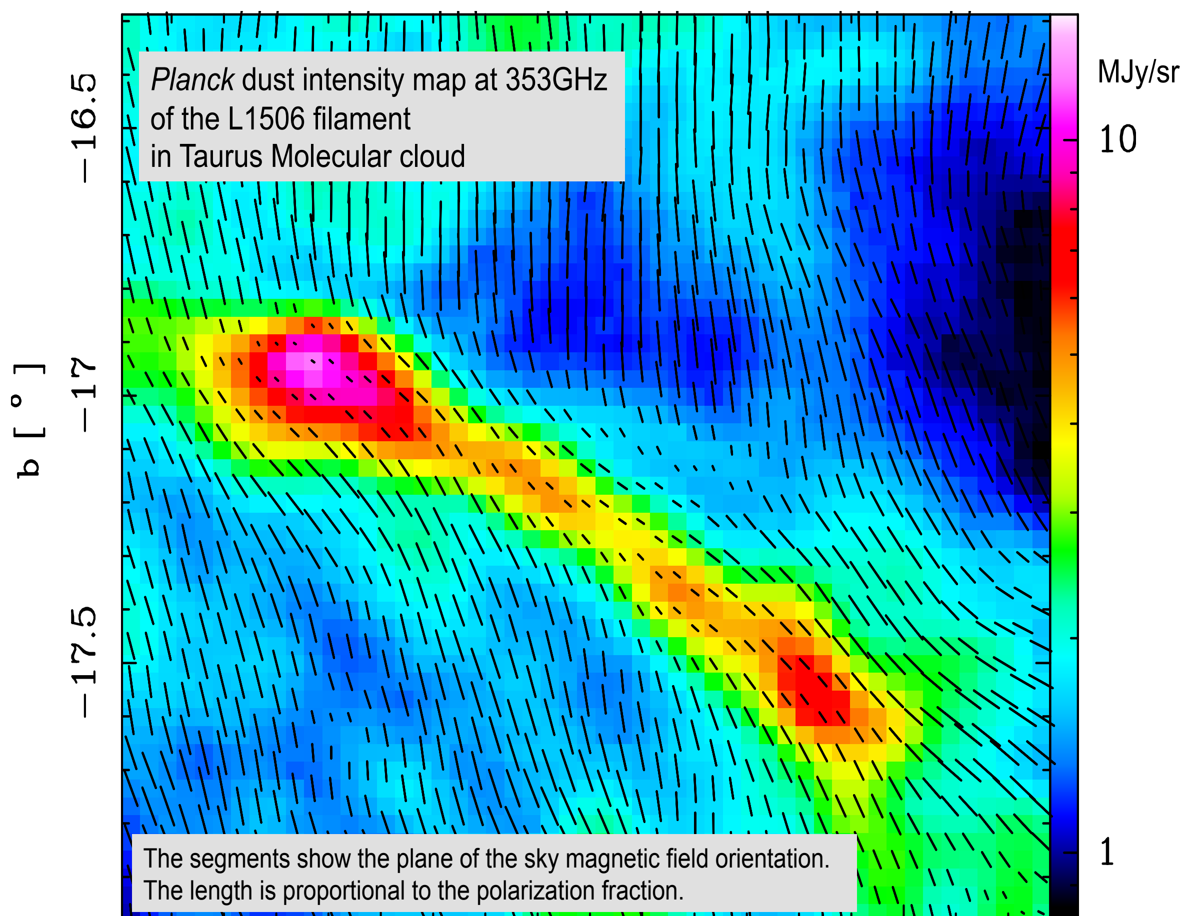

Planck total intensity at 353GHz (850μm) in MJy/sr
Segments: $\boldsymbol{B}_{POS}$ length ~ polarization fraction (10' resolution)

Modelling the magnetic field structure of a filament

Philosophy of the modelling:

- Initial gas density and magnetic field uniform
- Frozen-in conditions: magnetic field lines are dragged with the collapsing gas and concentrate towards the central part of the filament
- We consider a radially symetric configuration
- The "displacement law" satisfy the conservation of mass

$$\pi r_0^2 n_0 = 2\pi \int_0^r n(r')r'\mathrm{d}r'$$

Initial condition — Present state

Arzoumanian et al., in prep.

Present day (observed) radial density profile

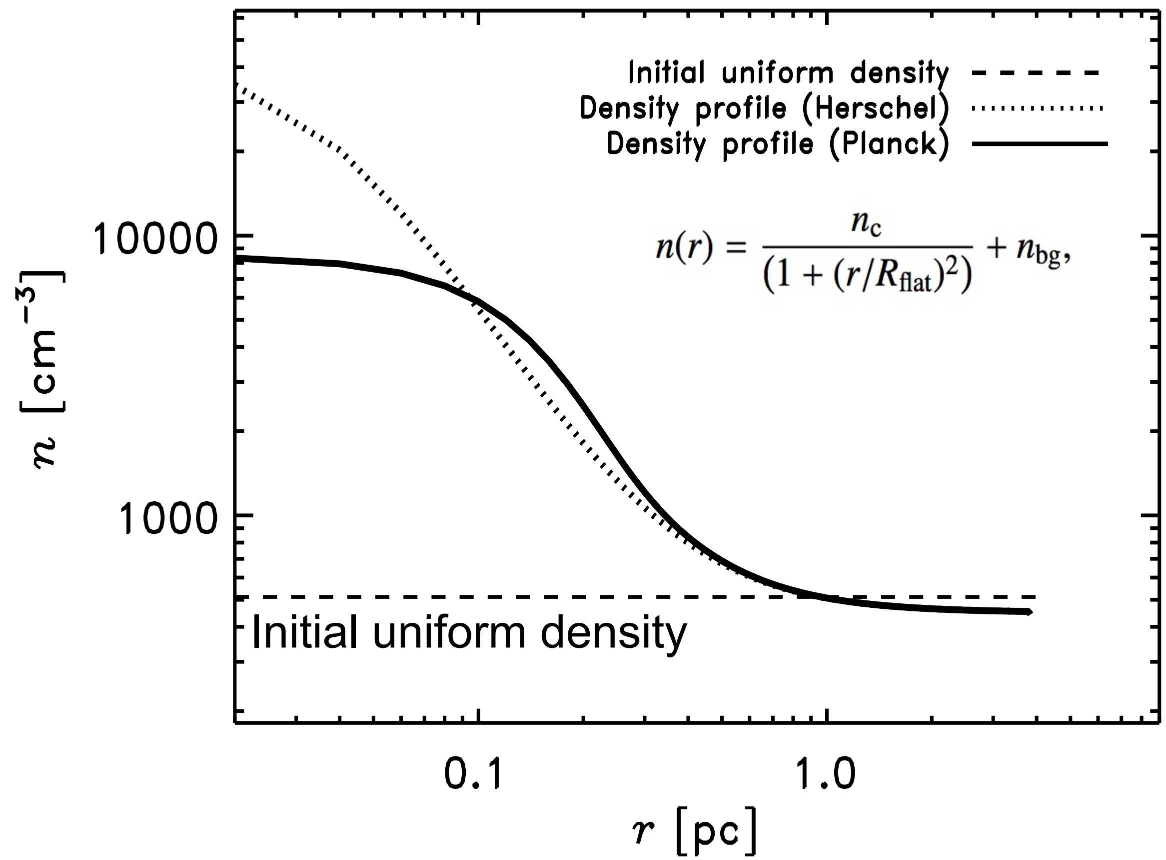

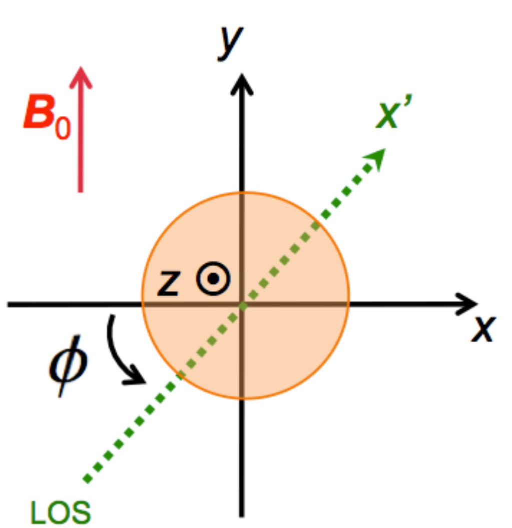

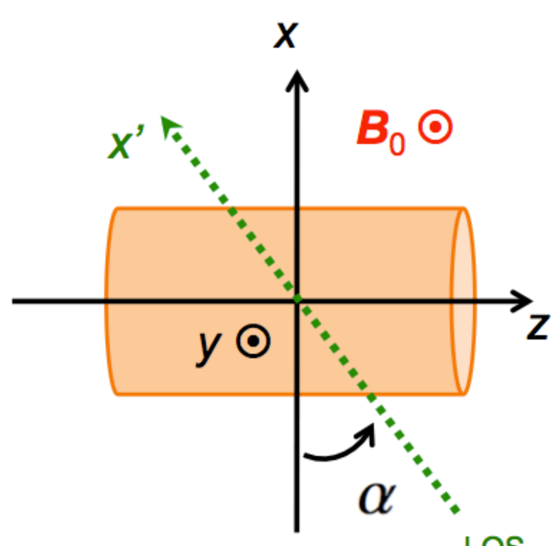

Initial magnetic field

$$\boldsymbol{B}_0 = B_{0x}\,\boldsymbol{e}_x + B_{0y}\,\boldsymbol{e}_y,$$

Present magnetic field

$$\boldsymbol{B} = \nabla \times \boldsymbol{A}$$

Vector potential

Modelling the magnetic field structure of a filament

Density map and $\boldsymbol{B}_{\mathrm{POS}}$ orientation

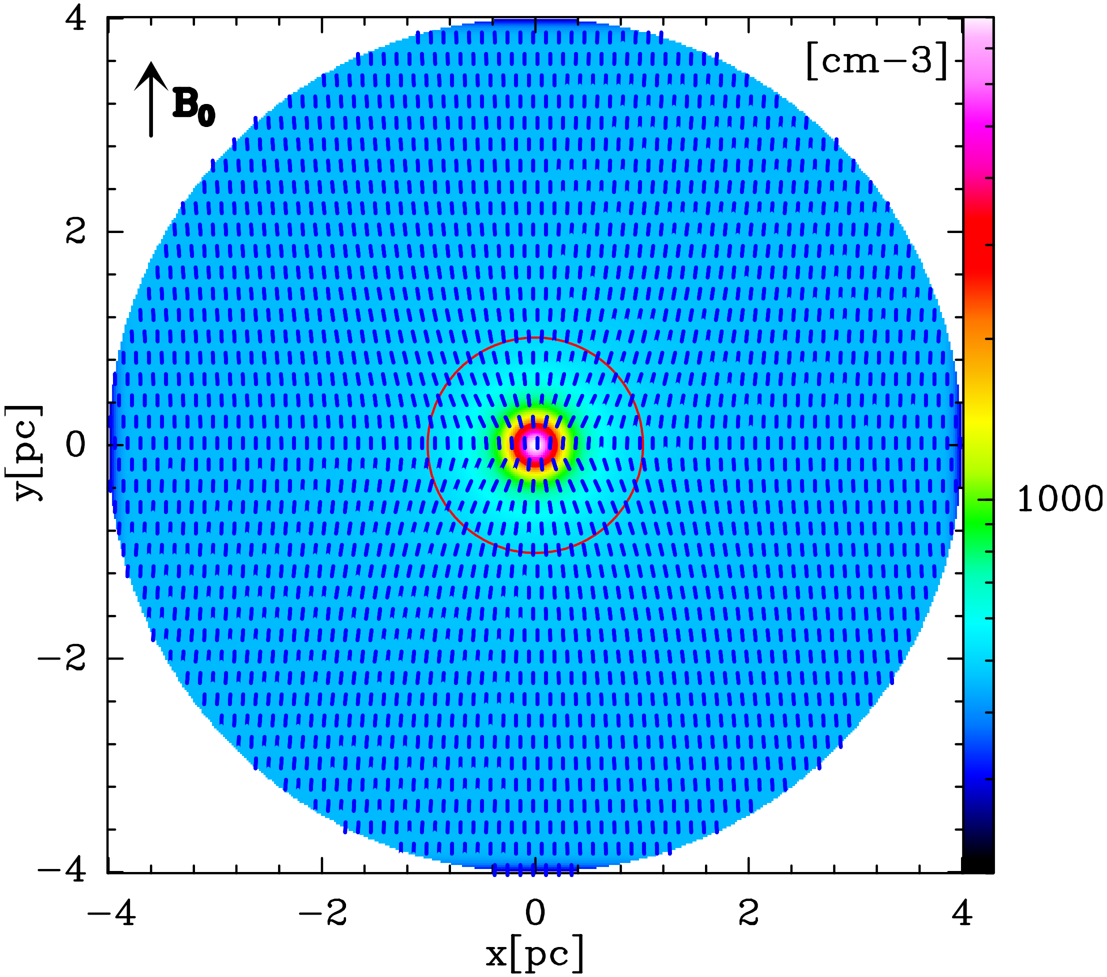

B field intensity and $\boldsymbol{B}_{\mathrm{POS}}$ orientation

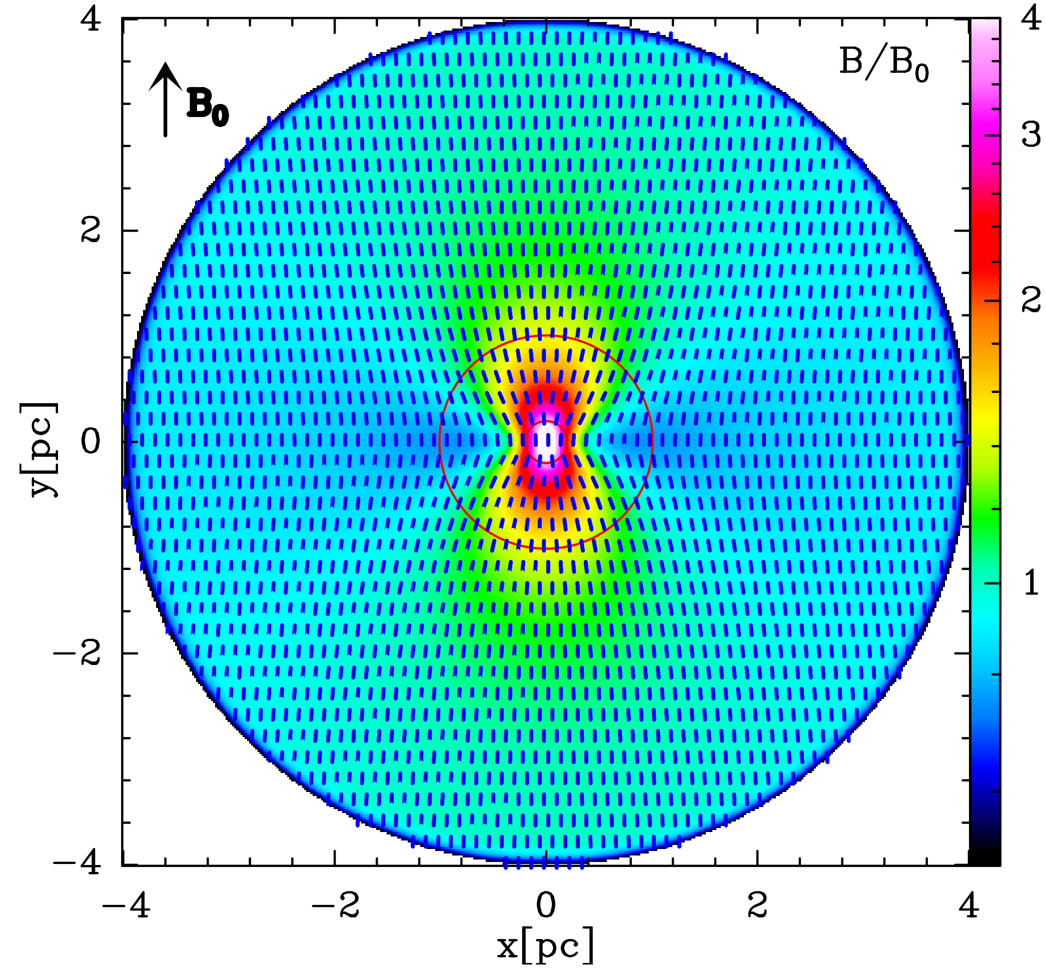

Face on view maps of the model filament + cloud

See also Tomisaka 2015, Auddy et al. 2017

I, Q, U from the modeled cube

$$I = \int S_\nu \mathrm{e}^{-\tau_\nu} \left[1 - p_0 \left(\cos^2 \gamma - \frac{2}{3} \right) \right] \mathrm{d}\tau_\nu;$$

$$Q = \int p_0 \, S_\nu \, \mathrm{e}^{-\tau_\nu} \cos(2\phi) \cos^2 \gamma \, \mathrm{d}\tau_\nu;$$

$$U = \int p_0 \, S_\nu \, \mathrm{e}^{-\tau_\nu} \sin(2\phi) \cos^2 \gamma \, \mathrm{d}\tau_\nu.$$

Polarization properties

$$P = \sqrt{Q^2 + U^2}$$

$$p = P/I$$

$$\psi = 0.5 \times \arctan(-U, Q).$$

Modelling the magnetic field structure of a filament

Polarization angle and fraction across the filament

Arzoumanian et al., in prep.

-We see both variation of the polarization angle and the decrease of the polarization fraction from the background to the filament as in observations

→ The "hour glass" magnetic field configuration may be responsible, at least partly, for the observed decrease of the polarization fraction in "dense" filaments

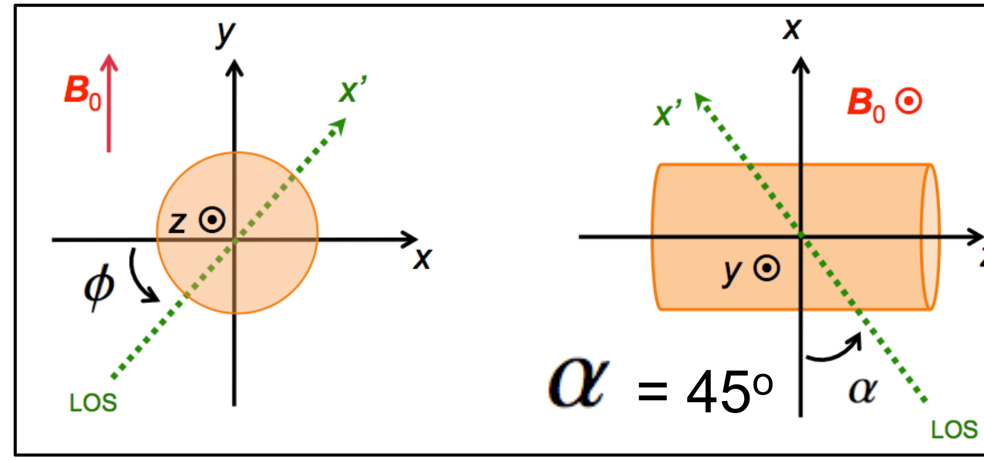

B_{POS} orientation across the filament

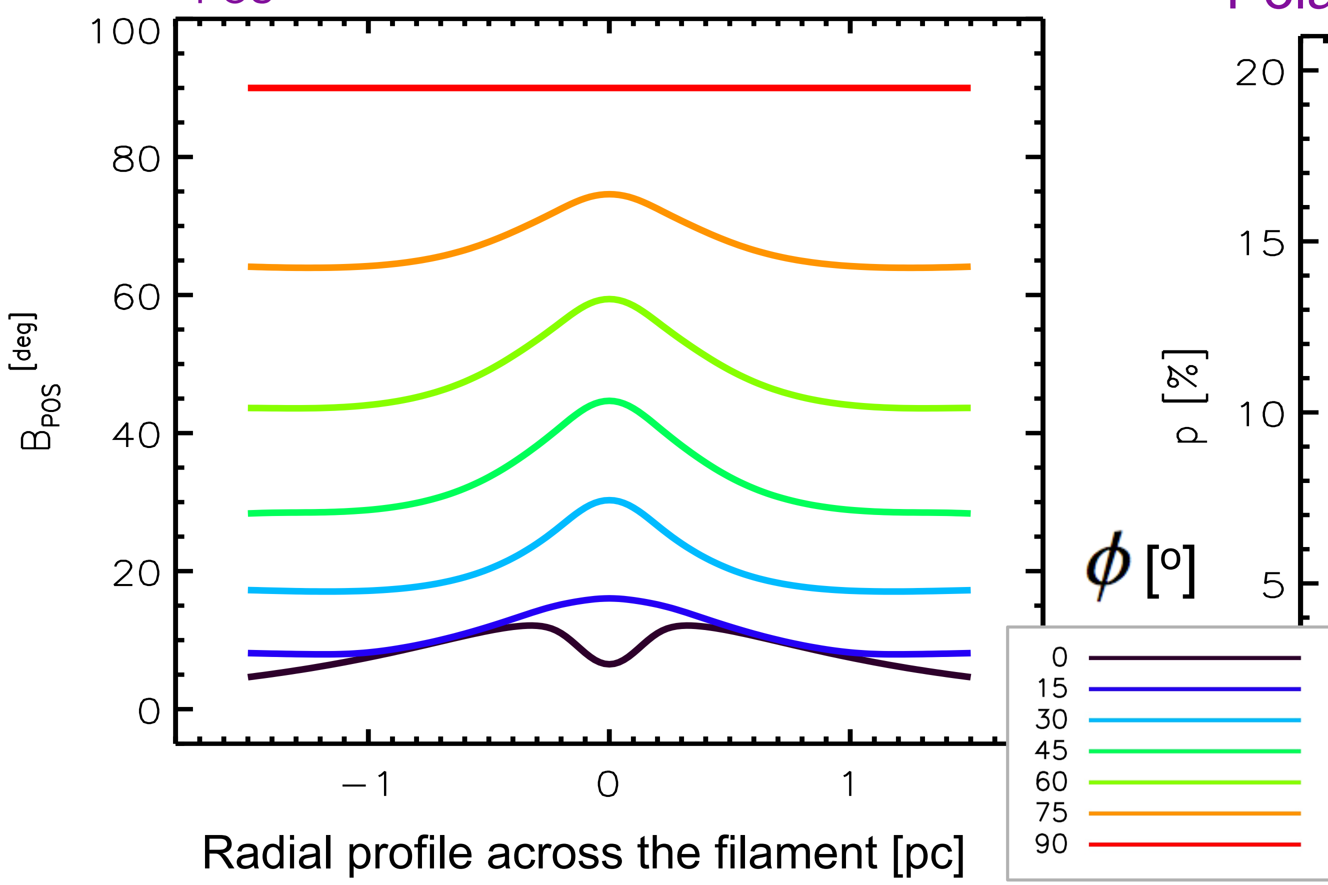

Polarization fraction across the filament

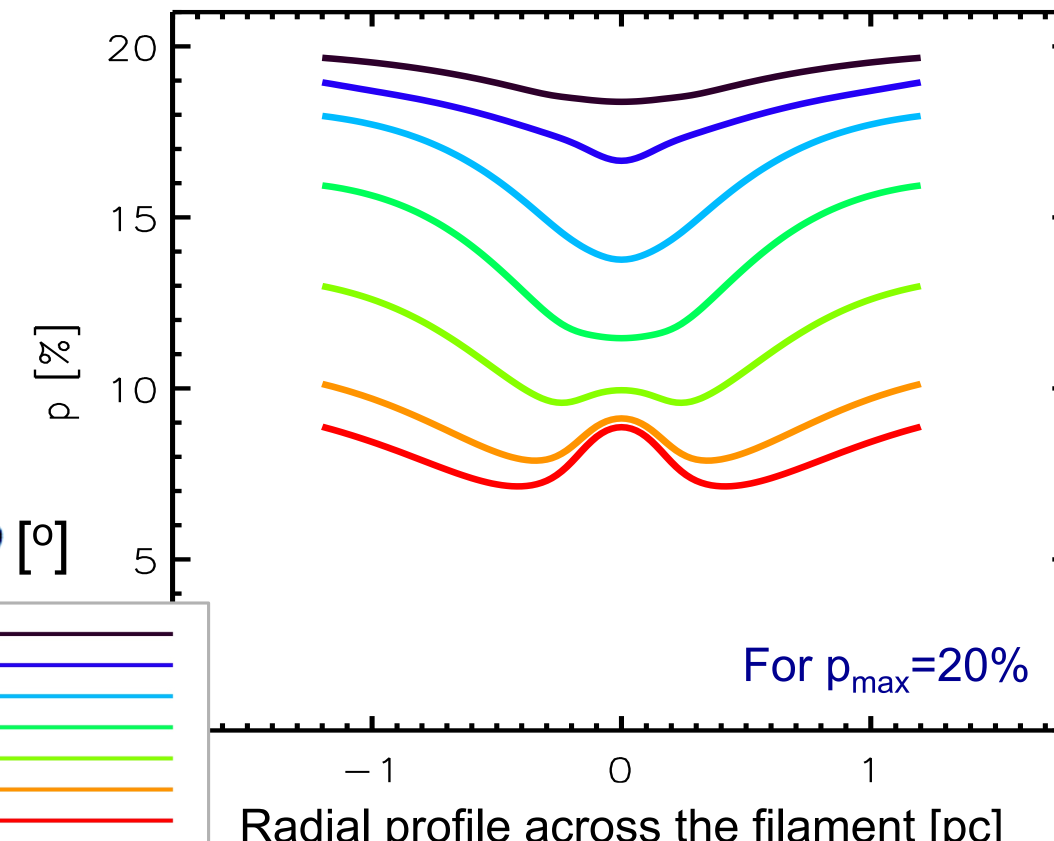

Doris Arzoumanian, MHD workshop, December 13, 2017, Kagoshima

Summary and conclusions

• The *Herschel* results support a “filamentary paradigm” for star formation, where 0.1pc-wide supercritical filaments are the main sites of star formation, and they may govern the star formation process.

• Multiple velocity components observed towards filaments may be linked to large scale structures/sheets interacting with the filament.

• The analyses of *Planck* dust polarization data (in the regime of optically thin dust emission) indicate that the observed scatter in polarization fraction and angle can be understood as a result of depolarization due to LOS integration and orientation of the mean B field with respect to the LOS.

• It is important to analyse simultaneously polarization angles and fractions: Both give us a hint on the magnetic field structure along the LOS.

• Modeling dust polarization towards supercritical filaments may give insights on their B-field, which is important to constrain their formation, evolution, and fragmentation into star forming cores.

Taurus (star forming cloud)